DISENTANGLING THE ROLES OF MOLECULAR GUIDANCE CUES AND SPONTANEOUS ACTIVITY IN THE EMERGENCE OF VISUAL TOPOGRAPHIC MAPS

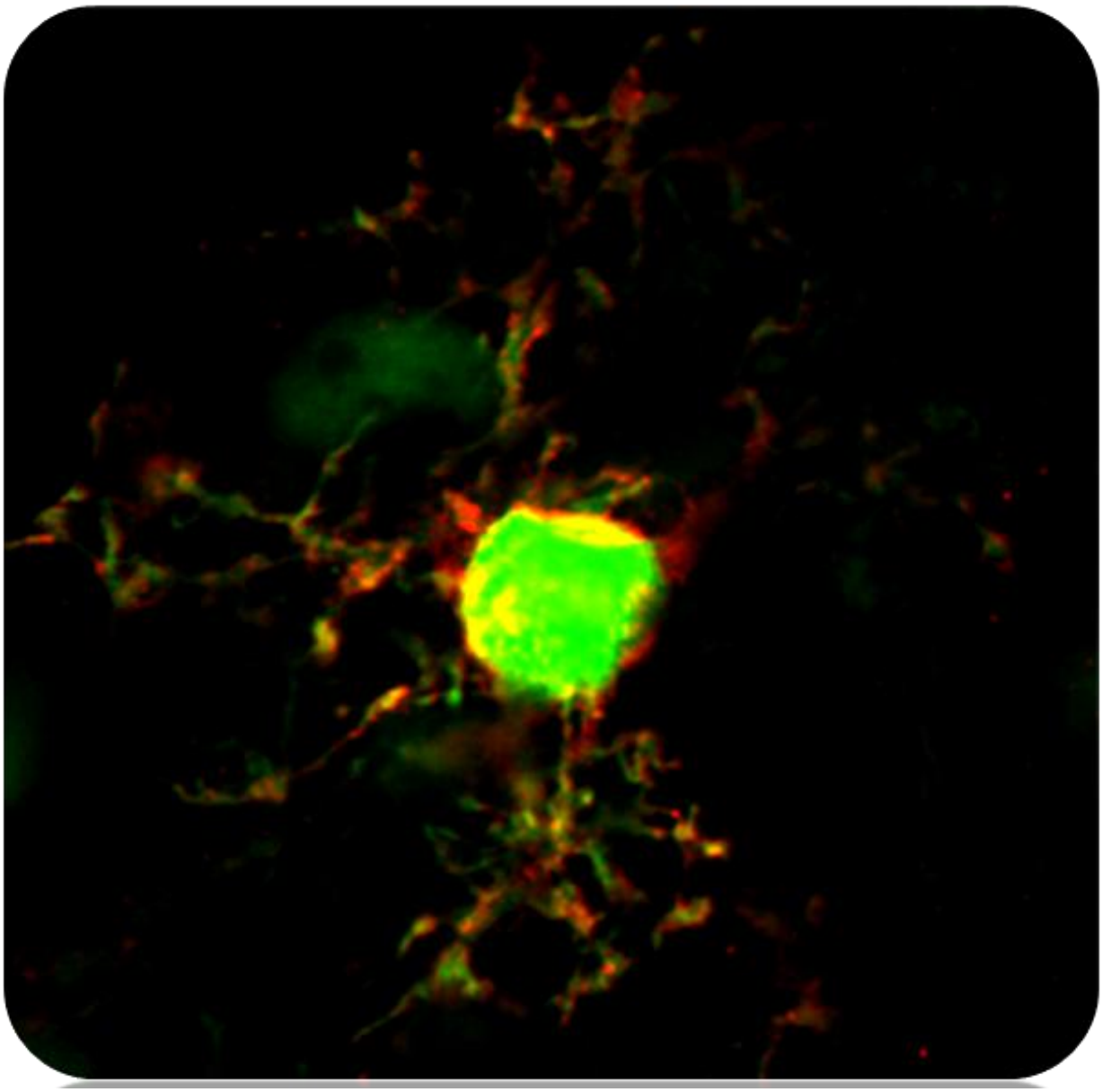

Isabel Benjumeda Wijnhoven

Advisors: Luis Martínez Otero and Eloísa Herrera

Instituto de Neurociencias de Alicante

INSTITUTO DE NEUROCIENCIAS

Consejo Superior de Investigaciones Científicas
Universidad Miguel Hernández
Instituto de Neurociencias

Prof. Juan Lerma
DIRECTOR

D. Juan Lerma Gómez, Director del Instituto de Neurociencias de Alicante, Centro Mixto de la Universidad Miguel Hernández (UMH) y de la Agencia Estatal Consejo Superior de Investigaciones Científicas (CSIC),

INFORMA:

Que la Tesis Doctoral titulada "Disentangling the roles of molecular guidance cues and spontaneous activity in the emergence of topographic maps" ha sido realizada por D. ª Isabel Benjumeda Wijnhoven, bajo la dirección de los Prof. Luis Martínez Otero - Eloísa Herrera González de Molina, y da su conformidad para que sea presentada a la Comisión de Doctorado de la UMH.

Y para que conste a los efectos oportunos, firma el presente certificado en San Juan de Alicante, a 22 de Octubre de 2012

Fdo. Juan Lerma
Director del Instituto de Neurociencias UMH-CSIC

direccion.in@umh.es
director.in@csic.es
www.ina.umh.es

Tel: +34 965-919221 (d)
+34 965-919220 (s)
Fax: +34 965 919561

Av Ramón y Cajal s/n
Campus de San Juan
03550 SAN JUAN DE ALICANTE– ESPAÑA

Consejo Superior de Investigaciones Científicas
Universidad Miguel Hernández
Instituto de Neurociencias

D. Luis M. Martínez Otero y D. Eloísa Herrera González de Molina, Científicos titulares del CSIC e investigadores de la plantilla en el Instituto de Neurociencias de Alicante, centro mixto CSIC-UMH,

CERTIFICAN,

Que D. Isabel María Benjumeda Wijnhoven, licenciada en Psicología, ha realizado bajo su dirección el trabajo experimental que recoge su Tesis Doctoral "Disentangling the roles of molecular guidance cues and spontaneous activity in the emergence of topographic maps".

Que los que suscriben han revisado los contenidos científicos y los aspectos formales del trabajo y dan su conformidad para su presentación y defensa públicas.

Para que así conste, y a los efectos oportunos, firman el presente Certificado en San Juan de Alicante, a 27 de Noviembre de 2012.

Fdo. Eloisa Herrera

Fdo.: Luis M. Martínez

http://in.umh.es/

Tel: +34 965-919210
+34 965-919209
Fax: +34 965 919561

Av Ramón y Cajal s/n
CAMPUS DE SAN JUAN
03550 SANT JOAN D'ALACANT– SPAIN

ACKNOWLEDGMENTS

ACKNOWLEDGMENTS

A mis jefes, por darme esta oportunidad y por todo el apoyo y la ayuda que e han restado. Por su paciencia y por creerme capaz de conseguirlo.

A mi familia, porque pese a no entender mucho de este mundo, a su manera me apoyaron y siempre me preguntaron con gran curiosidad por los ratones…

A mis compañeras, con los que he compartido sonrisas y lágrimas, frustraciones y alegrías, con las que he podido contar durante estos 4 años, desde aquel día en que comenzaron los cursos de doctorado en un lenguaje nuevo para mí,

A todos los que desde el principio me ayudaron a creer que esto seria posible y me contagiaron su energía y entusiasmo, la curiosidad y la ilusión, instándome a seguir adelante y a no tener miedo.

¡Gracias por ayudarme a llegar hasta aquí!

PREFACE

PREFACE

The work presented in this dissertation has been written for publication in the form of two articles, one of which is already submitted:

Isabel Benjumeda[1], Augusto Escalante[1], Geraud Chauvin[1], Joaquín Márquez[1], Guillermina López-Bendito[1], Luis Martínez[1]* and Eloísa Herrera[1]*. **Spontaneous activity is essential for branching and pruning but dispensable for neural specification, axon growth, pathfinding and map topography.** *Equal contribution. Submitted.

Isabel Benjumeda, Hector Hiero, Steve Macknik, Luis Martinez. **Patterns of retinal calcium imaging *in vivo* during the first postnatal week**. In preparation.

SUMMARY

SUMMARY

Prior to the onset of sensory experience neural circuits develop through a combination of genetic instructions and activity-dependent mechanisms. Classic studies supported a model in which axon guidance molecules and spontaneous activity act independently and sequentially to first guide axons to form a rough circuit at the target tissues which is then refined by clustering correlated inputs. Recent experiments have questioned this model proposing that spontaneous activity has a direct effect on axon guidance mechanisms in different developmental stages such as differentiation, axon guidance or map topography. Using the retinotopic map of mice as a model we have developed an experimental approach *in vivo* to block activity in a sustained and reliable way in retinal ganglion cells (RGCs) to definitively clarify the role of spontaneous activity during development and unravel the controversial question of whether or not it is required to activate the repulsive signaling mediated by EphA/ephrinAs during the formation of visual topographic maps.

In this study, we first performed calcium recordings in the developing retina of alive animals in order to analyze the patterns of retinal spontaneous activity *in vivo* during the first postnatal week and found calcium transients with a clear correlation between neighboring cells. Then we blocked spontaneous activity in embryonic RGCs *in vivo* (by ectopic expression of the inward rectifier potassium channel Kir2.1) and showed that differentiation, axonal growth and axon pathfinding are activity-independent processes in these neurons. In addition, contrary to previous studies *in vitro,* our results show that, although spontaneous activity is essential for local arborization of retinal axons in the termination zone (TZ) at the targets, it is dispensable for the activation of EphA/ephrinA signaling and therefore for topography, as predicted by the classic model.

INDEX

INDEX

Preface **9**

Summary **13**

List of figures **21**

Abbreviations **25**

Introduction **29**

1. Topographic maps 31

2. The visual system as a model to study topographic map formation 32

2.1 The formation of the retinocollicular map 36

2.2 Mechanisms involved in the formation of the retinocollicular map 38

2.2.1. Eph/ephrin signaling in retinocollicular map formation 38

i. The establishment of the retinocollcular map along the M-L axis 39

ii. The establishment of the retinocollicular map along the R-C axis 41

2.2.2. Spontaneous activity n retinocollicular map formation 46

2.2.3. Crosstalk between spontaneous activity and EphA/ephrinA Signaling 50

Aims **55**

Materials and Methods **59**

1. Optic Fiber calcium imaging *in vivo* 61

1.1. Animals 61

1.2 General surgical methods 62

1.3 Fibre-coupled confocal image analysis **63**

2. Electroporation *in utero* 64

2.1. Animals 64

2.2 General surgical methods 64

2.3 *In utero* electroporation 64
3. Immunohistochemistry 67
4. Two-Photon Imaging 67
5. Histology 69
5.1 Histological Imaging 69
6. Analysis of targeted axons in the SC 69
7. qRT-PCR 70
8. Axon arbor reconstruction in single cell electroporation 71

Results 73

1. Correlated firing of RGCs *in vivo* 75
2. Blockade of spontaneous activity in RGCs *in vivo* 78
3. Differentiation, axon growth or pathfinding are not altered after RGC activity blockade 81
4. Retinal spontaneous activity is not required to activate EphA/ephrinA signaling during retinocollicular map formation 85
5. Spontaneous activity is required for local remodeling of RGC axons once they are in the correct TZ 89

Discussion 91

1. Waves of spontaneous activity in the retina 93
2. Spontaneous activity is not required for differentiation, axon growth or pathfinding of RGCs 94
3. Spontaneous activity in the formation of the retinocollicular map 96

Conclusions 99

Bibliography 103

LIST OF FIGURES

LIST OF FIGURES

Figure 1. The wiring optimization principle.

Figure 2. Cell organization in the retina.

Figure 3. General view of the mammalian visual system.

Figure 4. Sagittal section of a mouse brain.

Figure 5. Retinotopic projection of the retina onto the SC.

Figure 6. Retinotopic map formation in differences species.

Figure 7. The guidance of pioneer axons in higher vertebrates is topographically inaccurate at birth.

Figure 8. Gradients of Eph/ephrinAs and Bs in the retina and the SC

Figure 9. Mapping abnormalities in ephrinA mutant mice (LOF) and GOF studies

Figure 10. Model representing the generation of retinal waves.

Figure 11. Changes in bursts of action potentials through the development of the retinal circuit.

Figure 12. Mice lacking the β2 subunit of the nicotinic acetylcholine receptor show no retinal waves during the first postnatal week.

Figure 13. Altered retinal waves produce defects in axon refinement.

Figure 14. Blockade of calcium entry *in vitro* by TTX prevents the collapse of growth cones from temporal RGCs in response to ephrinA5.

Figure 15. Spontaneous activity in the retina is required for the elimination of exuberant retinal axons in the SC *in vitro*.

Figure 16. Microscope used for surgery and optic fiberscope used for *in vivo* recordings.

Figure 17. Schematic representation of the microprobe insertion in the retina

Figure 18. Retina extraction after *in vivo* calcium recordings

Figure 19. Mouth controlled pipette system, paddle electrodes and electroporator.

Figure 20. Schematic representation of a micropipette and electrodes

Table 1. Optimal conditions for electroporation at different embryonic stages.

Figure 21. Two photon microscope and micromanipulator.

Figure 22. Example of analysis of targeted axons at the SC.

Figure 23. Raw data showing calcium imaging in a P8 retina

Figure 24. Statistics representing duration and magnitude of retinal calcium transients.

Figure 25. Correlation between RGCs placed near to each other in the retina.

Figure 26. Coexpression of Kir2.1 and EGFP in RGCs.

Figure 27. Ectopic expression of Kir2.1 blocks calcium transients in RGCs.

Figure 28. Cell survival is not altered after RGC activity blockade.

Figure 29. Axon growth and guidance are not altered after RGC activity blockade.

Figure 30. Axons from RGC expressing Kir2.1 correctly reach the caudal SC at birth.

Figure 31. Activity blockade leads to disruption of the visual topographic map.

Figure 32. Spontaneous activity is not required for the endogenous expression of retinal EphA5 and EphA6 mRNAs.

Figure 33. Ectopic expression of EphA6 in the central retina reproduces the endogenous pattern of temporal axons

Figure 34. Spontaneous activity is not required for activating the EphA/ephrinA signaling during retinocollicular map formation.

Figure 35. Spontaneous activity is required for proper remodeling of RGC axons but not for topography.

Figure 36. Drawing illustrating the two-phase process during the formation of the retinocollicular map and the main mechanisms driving each step.

ABBREVIATIONS

ABBREVIATIONS

Ach Acetylcholine

AchR Acetylcholine receptor

A-P Anterior-posterior

AP Action Potential

β2 Beta 2 subunit

Ca^{2+} Calcium

ChAT CholineAcetyltransferase

CNS Central Nervous System

C-R Caudal - rostral

DIV Days *in vitro*

D-V Dorsal-ventral

GPI Glycosylphosphatidylinositol

KO Knock out

L Lateral

LGN Lateral Geniculate Nucleus

M Medial

N Nasal

nAchRs Nicotinic acetylcholine receptors

N-T Nasal - temporal

RGC Retinal Ganglion Cell

SC Superior Colliculus

T Temporal

TTX Tetrodotoxin

TZ Termination zone

WT Wild Type

INTRODUCTION

1. Topographic maps

Most neural circuits in the brain of higher vertebrates are spatially organized, giving rise to what is known as topographic maps. One of the most famous examples of a topographic map is the retinotopic organization of the visual system by which nearby neurons in the different visual areas receive and process inputs that originate in nearby retinal ganglion cells. Similar ordered arrangements are pervasive, occupying much of the neocortex of all mammalian species, both in motor and sensory structures.

There are developmental, anatomical and functional reasons for the emergence of topographic maps. First, they are the most parsimonious way of transferring spatially structured information from one group of neurons to the next, possibly keeping to a minimum the need for different guidance mechanisms through development (Tessier-Lavigne and Goodman, 1996). Second, topographic maps effectively group together neurons that are functionally related permitting synaptic partners to interact over short axonal and dendritic pathways (Allman and Kaas, 1974) which largely reduces signal delays and attenuation (Rall et al, 1992; Rushton, 1951). And, third, wiring distant neurons in the brain is metabolically costly to an organism and increases the volume taken up by the nervous system (Mitchison, 1991; Cherniak, 1992; Ramón y Cajal, 1999; Attwell and Laughlin, 2001; Chklovskii and Koulakov, 2004). Thus, having connected neurons as close as possible is most evolutionarily robust and, therefore, more likely to be selected. This argument is known as the “wiring economy principle” and derives from the laws of economy of time, space and conductive matter proposedby Ramón y Cajal in the nineteenth century (Chklovskii and Koulakov, 2004) (Fig. 1).

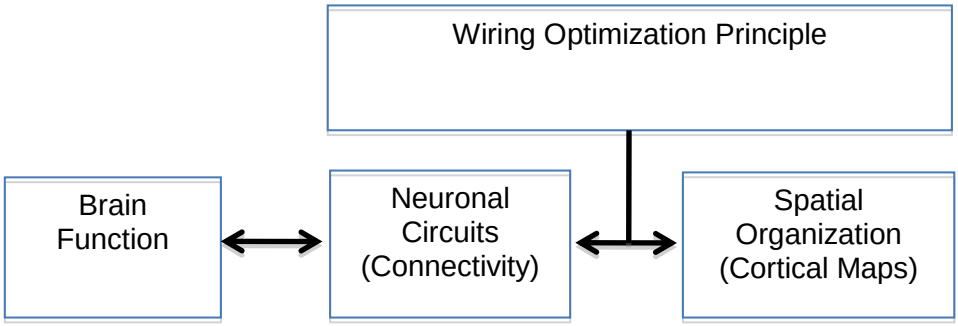

Figure 1. The wiring optimization principle. This principle establishes a link between neuronal circuitry and neuronal spatial organization and predicts a model in which topographic maps are the most economic form of circuit organization.

2. The visual system as a model to study topographic map formation

Given the importance of topographic maps for the correct functioning of the nervous system, it has been a major focus of developmental neurobiology over the past decades to work out the mechanisms by which topography is set up. Among the different topographic maps in the brain, the visual system has revealed over the years as an excellent model to study formation of topographic neural maps thanks to its particular anatomy and accessibility.

Visual information is perceived by the retina and sent to the brain to be processed. The retina has a thickness of approximately 250 µm, with three sheets of neuronal bodies separated by two layers holding the synapses made by the axons and dendrites from those neurons (Hubel, 1988). During development, the retina forms as an outpocketing of the diencephalon called the optic vesicle. The inner wall of the optic cup leads to the retina and the outer wall gives rise to the retinal pigment epithelium, which closely interacts with photoreceptors reducing the scattered light that reaches the retina providing it with metabolic support. Cells in the ventricular zone undergo successive periods of proliferation and differentiation to generate seven types of retinal cells in a precise order (six types of neurons and one glial cell type). The vertebrate

neural retina is patterned along all its axes and retinal differentiation initiates in the central retina, expanding to the periphery, with ganglion, amacrine and horizontal cells originating first and rods, bipolar and Müller glia cells differentiating last. Therefore, the neural retina is a complex nervous structure made up of a number of ordered layers with different functions (Fig. 2) (Cepko et al., 1996).

Light coming from the outside world is projected onto 125 million of photoreceptors in the retina. These photoreceptors, called rods and cones, are specialized in the transmission of electrical signals that are filtered by the three classes of retinal interneurons; horizontal, bipolar and amacrine cells. These interneurons transmit visual information to retinal ganglion cells (RGCs). Each RGC receives input from many bipolar cells and each bipolar cell is fed by a similar number of photoreceptors (Huberman and Niell, 2011)

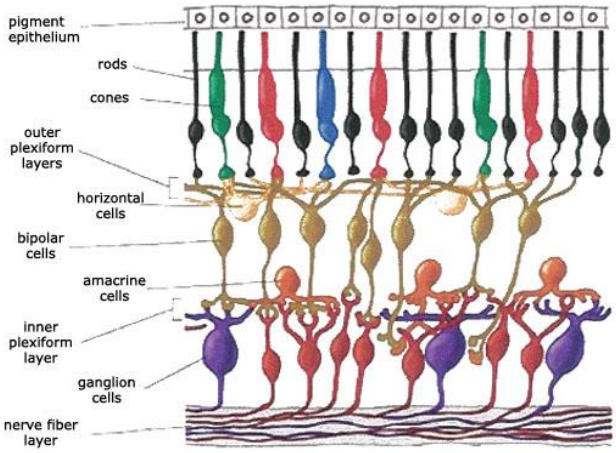

Figure 2. Cell organization in the retina. Light is projected into rods and cones and then filtered by the three major classes of retinal interneurons; horizontal, bipolar and amacrine cells which in turn convey visual information to RGCs. (Adapted from the *Scientific Research Society)*

RGCs are the only retinal cell type that extends axons out of the retina to transmit visual information up to the brain. In mammals RGC axons exit the eye at the optic disc, travel along the base of the ventral diencephalon toward the midline where they meet axons from the contralateral eye and form the optic chiasm. At the chiasm a portion of axons cross the midline to project to the contralateral targets in the thalamus

(into the lateral geniculate nucleus, LGN) and in the superior colliculus (SC), while a different axonal population grows away from the midline to project to ipsilateral targets. Projections to the thalamus occur in a topographic manner which appears imprecise at the time of establishment but undergoes a refinement process as the system matures and before first sensory input. Second-relay thalamic axons grow into the subcortical telencephalon during embryonic development to further reach the visual cortex, where sensory information coming from both eyes is processed (Reviewed in Erskine and Herrera, 2007) (Figure 3).

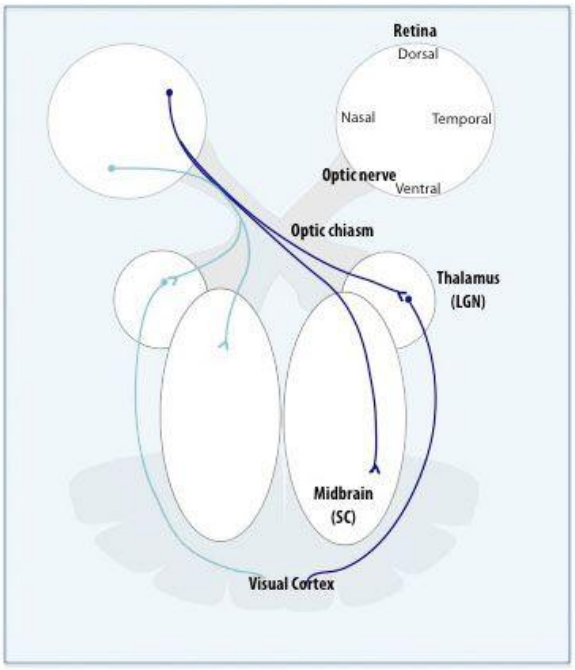

Figure 3. General view of the mammalian visual system. RGC axons (blue lines) exit the retina via the optic nerve to the optic chiasm where they cross (contralateral axons; dark blue line) or avoid the midline (ipsilateral axons; light blue line). From there they project topographically to the main visual targets in the brain: the LGN in the thalamus and the SC. Second-relay neurons from the thalamus then send visual information to the visual cortex.

In the SC, which is a prominent structure visible on the dorsal surface of the midbrain (Fig. 4), RGC axons also project in a topographic manner. As in the LGN, the retinocollicular map (retinotectal in non-mammalian vertebrates) is not precisely established from the beginning but its development is roughly finished before photoreceptors can transduce light (Reviewed in Huberman, 2008). The SC coordinates head and eye movements, mediates reflexive eye movements, head turns

and shifts of attention. This structure is present in all vertebrates and it is usually described as a visual reflex centre with a layered organization.

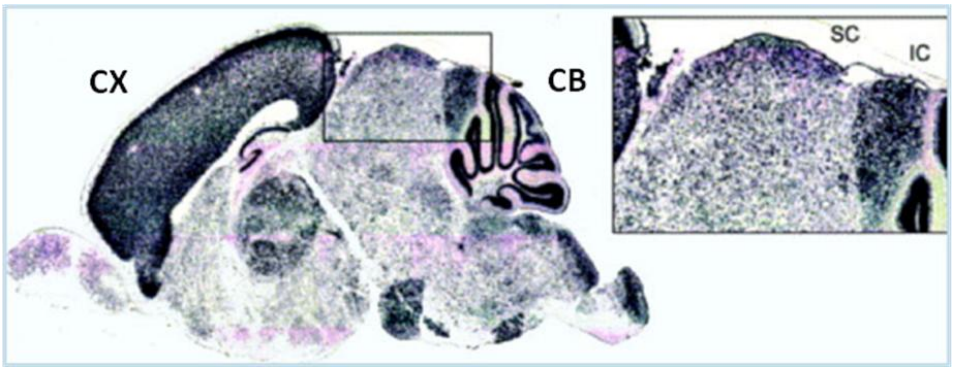

Figure 4. Sagittal section of a mouse brain. Nissl staining showing location of the SC, between the Cortex and Cerebellum. On the right, close-up image of the squared area representing the SC and the IC. CX Cortex, CB Cerebellum, IC Superior Colliculus (Adapted from *Plas et al., 2004*).

In the retinocollicular map, orthogonal nasal-temporal and dorsal-ventral axes of the retina are mapped onto the orthogonal caudal-rostral and lateral-medial axis of the SC (Lemke and Reber, 2005) in such a way that the termination zone (TZ) for a particular axon in the SC corresponds to the topographic location of its RGC body into the retina (Godement et al., 1984; Nakamura and O'Leary, 1989). Thus, as in the LGN, in the SC visual projections two neighboring RGCs are connected to two adjacent points in the target field. This topographic arrangement allows the projection of a continuous image of the visual field onto the surface of the target structure (Cang et al., 2008) (Fig. 5).

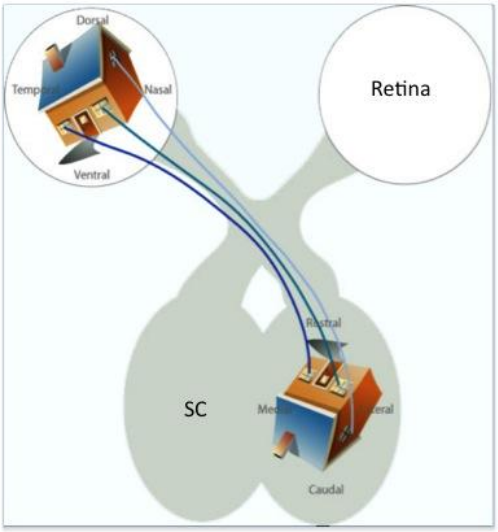

Figure 5. Retinotopic projection of the retina onto the SC. The retinocollicular projection is highly organized, in a way that axons from neighbouring neurons in the retina terminate in neighbouring positions in the SC. Axons originating in the nasal retina terminate in the caudal SC, while temporal RGCs send axons to the rostral SC. In addition, axons originating in the dorsal retina map to the ventral SC, while ventral RGC axons terminate in dorsal SC.

2.1 The formation of the retinocollicular map.

As other topographic maps, the retinocollicular map in the adult is different than that observed at birth. However, the maturation process that gives rise to the adult map shows important differences between frogs and fish on the one hand and chicks and rodents on the other. In frogs and fish, RGC axons extend directly to the correct location of their TZ. As the growth cone of the primary RGC axon reaches the location of its future TZ, it stops and starts to form short terminal branches at or near the base of the growth cone, which often acquires a branch-like morphology, and together they elaborate a local terminal arborization of the distal part of the primary axon (Harris and Holt, 1987; Kaethner and Stuermer, 1992; O´Rourke et al., 1994). The sizes of individual arbors along the A–P axis are relatively larger in the tectum of frogs and fish than in the tectum of chicks and the SC of mice. This is partly due to the fact that the RGC axons of frogs and fish reach the tectum and arborize at an early stage of tectal neurogenesis when the tectum is very small and only rostral tectum has been

generated. Therefore, in frogs or fish, their RGC axonal arbors are disproportionately large compared to the tectum during the early stages of tectal neurogenesis, and cover a greater percentage of its surface area than at later stages. In frogs and fish, arbors cover progressively less of the A–P axis as map development advances because the tectum expands substantially more than the arbors and some arbor refinement occurs (Debski and Cline, 2002). In contrast, the OT/SC of chicks and rodents expand relatively little over the period of map development (Fig. 6).

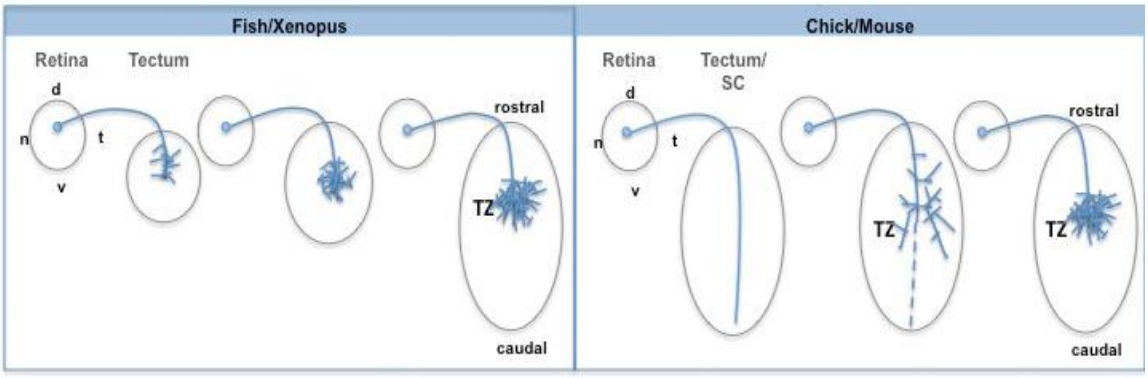

Figure 6. Retinotopic map formation in different species. In frog and fish, the tectum and retina expand throughout the development of the retinal projection. The tectum is much smaller in relation to a typical growth cone in frog and fish than in chick and mouse. RGC axons extend into the tectum and elaborate many small branches from the base of the growth cone. Arbors elaborate from these backbranches. In mouse and chick, RGC axons enter the OT/SC and initially extend posterior to the location of their future TZ. This initial axon overshoot is later eliminated while branches elaborate complex arbors at the TZ.

The development of the retinotopic map in the chick tectum and the rodent SC is a much complex process (Nakamura and O'Leary, 1989; Simon and O'Leary, 1992; Hindges et al., 2002). In an initial phase, RGC axon growth cones enter the target and extend posteriorly to their future TZ. Interstitial branches start forming at the AP position of the future TZ and extend preferentially along the latero-medial (L-M) axis toward their future TZ. At the same time, the primary axon retracts to the precise point that corresponds to the topographic location of the RGC in the retina, marking this way the region of the future TZ (Simon et al., 1992; Hindges et al., 2002; McLaughlin et al.,

2003). Therefore, the precise TZ where the axon turns to arborize in superficial layers (which is what we call topography) is determined at this stage (Phase 1; Topography phase). In a second phase, major segments of RGC axons that are distal to the appropriate TZ are eliminated, together with branches and arbors that formed at topographically incorrect positions. Complex arbors form then at the TZ (Phase 2; remodeling at the TZ) (Nakamura and O'Leary, 1989). This is therefore a local phase of axon remodeling at the TZ (Fig. 7).

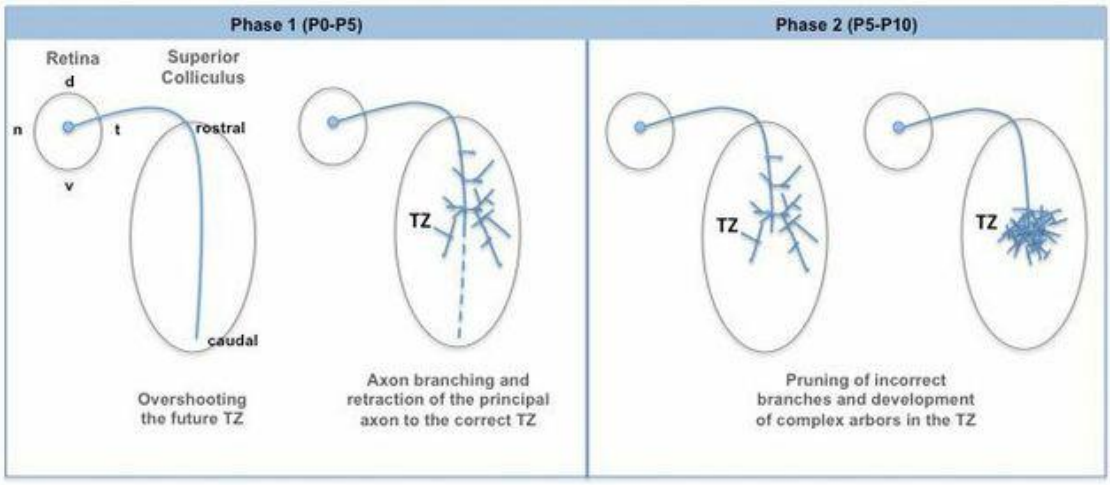

Figure 7. The guidance of pioneer axons in higher vertebrates is topographically inaccurate at birth. In mice, RGC axons enter the SC around P0 and overshoot the location of their future TZ after which the principal axon retracts. Interstitial branches form along the axon shaft in a distribution biased for the antero-posterior location of the TZ (Phase 1). In the remodeling phase (Phase 2) extensive pruning of incorrect branches takes place while a complex arbors forms in the correct TZ.

2.2 Mechanisms involved in the formation of the retinocollicular map

The development of the retinal pathway that finally generates a mature map at the main visual targets coincides with the expression of certain classes of axon guidance molecules (in particular Ephs/ephrins) and with the moment of development in which spontaneous activity takes place. Genetic instructions and activity-dependent mechanisms are both known to be essential for precise topographic map formation in the mammalian visual system. However, it is still unknown whether or not molecular

guidance cues and neural activity interact.

2.2.1. Eph/ephrin signaling in retinocollicular map formation

In 1963 Roger Sperry proposed the chemoaffinity theory to explain how retinal axons project topographically in the SC. Sperry cut the optic nerves of newts and rotated their eyes 180º, and observed that after regeneration of retinal axons to the tectum, the operated animals behaved as if they saw the world upside down and from back to front. After this unexpected result Sperry proposed that retinal cells must carry positional chemical labels (or chemoaffinity tags) that would determine their correct tectal terminations (Sperry, 1963). Some decades later, Bonhoeffer and his colleagues demonstrated the existence of a chemorepellent signaling in the caudal tectum that would guide the ordered projection of RGC axons along the temporal nasal (T - N) axis of the retina. Temporal RGC axons showed predilection for rostral tectal membranes (Walter et al., 1987), while RGCs from the nasal retina showed no preference for rostral versus caudal membranes (Walter et al., 1987; Cox et al., 1990). The authors further demonstrated that the chemorepellent activity of the caudal tectal membranes was associated with a protein attached to the membrane surface, ephrinA5 (Stahl et al., 1990; Drescher et al., 1995). These caudal tectal chemorepellents were presumed to be sensed by a receptor, or receptors, preferentially expressed by RGCs in the temporal retina, the EphAs.

Both ephrins and their receptors are divided into two groups, ephrinAs and Bs. EphAs are transmembrane proteins activated after their binding to the appropriate ephrin ligand. EphrinAs are attached to the cell membrane via a glycosylphosphatidylinositol (GPI) anchor and, together with their receptors, are expressed in gradients in the SC and the retina (Feldheim et al., 1998). Interactions between Eph receptors and their ephrin ligands require cell-cell contact and their binding mediate the repulsion of the axon that express the receptor. EphA receptors bind and are activated by only ephrin-As, and EphBs by only ephrinBs, with the

exception of EphA4, which binds both ephrinAs and -Bs (Brambilla et al., 1995; Gale et al., 1996). *In vitro* and *in vivo* approaches have now demonstrated that ephrinB/EphB signaling is involved in medial-to-lateral axis mapping while ephrinA/EphA signaling governs the mapping along the posterior-to-anterior axis in the SC.

i. The establishment of the retinocollicular map along the M-L axis.

In the retina, EphB receptors are expressed in an increasing dorsal-to-ventral gradient, while EphrinB1 is expressed in an increasing lateral-to-medial gradient in the SC and EphrinB3 is strongly expressed at the collicular midline. *EphB2/B3* double mutants show abnormal projections along the lateral-to-medial axis of the SC and the replacement of the kinase domain and C-terminus of EphB2 with LacZ lead to an equivalent or even more severe phenotype than the double knock-out of *EphB2/B3* (Hindges et al., 2002). The transcription factor ventral anterior homeobox encoded gene 2 (Vax2) is expressed in the developing mouse retina in a steep high ventral-to-low dorsal gradient and a shallower high-nasal-to-low-temporal gradient (Mui et al., 2002). In *Vax2* mutants, the expression of EphB2/B3 is reduced in ventral retina and RGCs projecting to the ventral thalamus display a shift in their termination zones from medial to lateral which is more severe than the defects in *EphB2/B3* double mutants, making Vax2 a presumably upstream regulator of EphB expression. These results together demonstrated an essential role of EphB/ephrinB signaling during the establishment of topography across the L-M axis of the retinocollicular map.

EphrinB1 signaling in medial to lateral topographic mapping seems to be counterbalanced by the action of Wnt3, originally known as a morphogen but apparently displaying guidance molecule character in the SC (Schmitt et al., 2006). *In situ* hybridization studies revealed a high medial to low lateral expression of *Wnt3* in mouse SC, similar to the expression pattern of ephrinB1. In a cell-culture assay, Wnt3 was shown to repel dorsal and ventral RGC axons at higher concentrations but acted growth stimulating on dorsal but not on ventral RGC axons at lower concentrations.

Ectopic Wnt3 expression in chick tectum repelled ventral axon termination zones thereby confirming the repulsive action of Wnt3 demonstrated in culture. This Wnt3 induced repulsion of axonal growth involved signaling via the Ryk receptor. *Ryk* is expressed in a high ventral to low dorsal gradient in the mouse retina and the expression of dominant-negative Ryk in dorsal chick RGCs led to a medial shift of RGC termination zones in the tectum. On the other hand, the Wnt3 induced stimulation of axon growth was shown to be mediated by Frizzled receptors, as this action could be blocked by application of secreted frizzle-related protein 2 (sFRP2). Therefore, the current model suggests that the repulsive Wnt-Ryk pathway competes with the attractive Wnt-Frizzled interaction to actively titrate the response to graded Wnt3 expression which, in turn, counterbalances the ephrinB1/EphB signaling (Fig. 8).

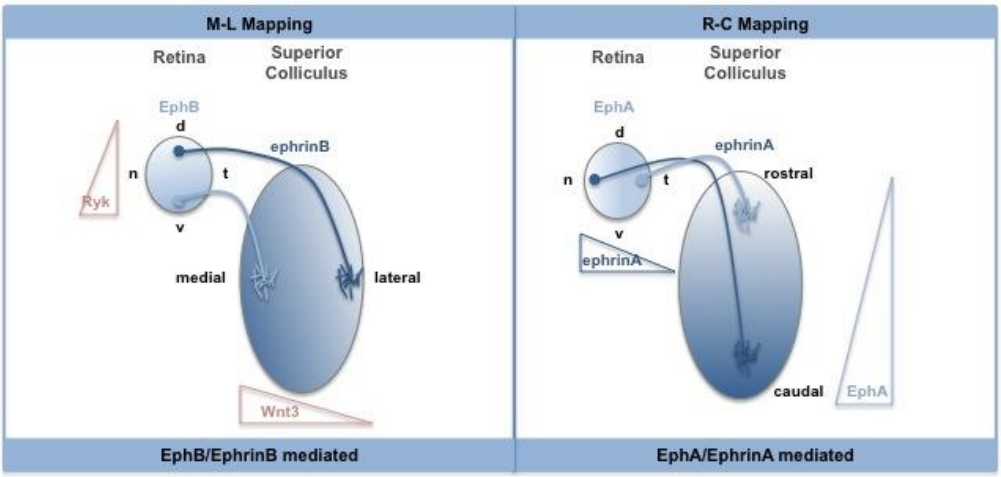

Figure 8. Gradients of Eph/ephrinA and Bs in the retina and the SC. In the left panel: Mapping in the M-L axis is mainly mediated by an EphB gradient (D<V) in the retina and the corresponding ephrinB (L<M) gradient in the SC and Ryk (D<V) and Wnt3 (L<M) gradients in the retina and SC respectively (pink triangles). In the right panel: Two gradient systems in the retinocollicular projection are involved in topographic mapping in the R-C axis. First, the EphA gradient in the retina (N<T) and the corresponding ephrinA gradient in the colliculus (R<C) (blue gradient), and second, the ephinA gradient in the retina (N>T) and the EphA gradient in the tectum (R<C) (represented by blue triangles).

ii. The establishment of the retinocollicular map along the R-C axis.

RGCs from different species express EphA receptors in a temporal (T) > nasal (N) gradient, whereas SC cells express the ephrinA ligands in a caudal (C) > rostral (R)

gradient (Fig. 8). In the mouse, a decreasing gradient of expression of the receptors EphA5 and EphA6 is found from temporal to nasal axons in retina while the ligand ephrinA5 is expressed in an increasing gradient from anterior to posterior SC and the ligand ephrinA2 displays the highest expression midway through the posterior half of the SC decreasing anteriorly and posteriorly (reviewed in Wilkinson, 2000).

Genetic loss of function experiments in mice have evidenced that EphA/ephrinA repulsive signaling is essential for mapping along the R-C axis. In mice deficient for *ephrinA5* temporal axons project more posteriorly in the SC and a proportion of axons transiently overshoot the IC (Frisen and Yates, 1998). In mice lacking ephrinA3 more posterior terminations of temporal axons are observed (Feldheim et al., 2000). Double homozygotes of *ephrinA2/ephrinA5* mice display striking mapping defects with temporal axons terminating more posteriorly and nasal axons more anteriorly than usual. Despite these mapping defects, RGC axon projections still fill out the complete SC.

Although these mutant phenotypes evidence a crucial role of the EphA/ephrinA signaling in R-C mapping they also demonstrate that additional mechanisms must be involved in the establishment of the retinocollicular map. The mutant phenotypes could be partly explained by a model of desensitization of EphA receptors via interactions with their ligands in the retina. It has been shown that the ligand ephrinA5 is expressed in a decreasing nasal-to-temporal gradient in mouse retina (Marcus et al., 1996) and it is possible that an overlapping expression of ephrinA/EphA in the nasal retina decreases the sensitivity of nasal axons to ephrinAs expressed in SC thereby creating a decreasing temporal-to-nasal gradient of “sensitive” EphA receptors. In fact, a cis interaction between ephrinA5 and EphA3 that results in the silencing of EphA3, has been recently demonstrated (Carvalho et al., 2006). The model of combined repulsion and competition of nasal and temporal axons for termination zones in the SC might also explain the difference in the degree of more anterior projections in *ephrinA2/A5*

double and *ephrinA5* single mutants as well as the fact that RGC projections still fill up the SC when ephrin gradients are disturbed (Feldheim et al., 2000). According to this model, temporal axons are unable to terminate in posterior SC because of repelling ephrins and are forced to terminate in the anterior part of the SC. On the other hand, nasal RGC axons are less sensitive to repulsing ephrin signaling and therefore can project to the posterior part of the SC. EphrinA/EphA reverse signaling (EphrinA playing as a receptor and EphA as the ligand) may also be an important mechanism in the establishment of topography. EphA7 is expressed in a reversely oriented gradient to the ephrinAs in the mouse SC and it is not expressed in the retina (Rashid et al., 2005). *In vitro*, retinal axons are repelled from EphA7 containing stripes and mutant mice display a disrupted retinocollicular map with nasal and temporal axons forming additional or extended termination zones, respectively.

A significant number of different molecules have been described to influence and interact with EphA/ephrinA function during retinocollicular map formation. For instance the, Brain-derived Neurotrophic Factor (BDNF) and its receptors TrkB and p75 neurotrophin receptor (NTR), together with the cell adhesion molecules L1 and CHL1 have been reported to indirectly modulate ephrin-A and influence R-C mapping (Feldheim and O´Leary, 2010). BDNF has been proposed to be a candidate for branching signaling (O'Leary et al. 1999; McLaughlin and O'Leary, 2005) promoting interstitial branching *in vitro* through a mechanism dependent on TrkB signaling (Choi et al., 2000). The transmembrane adhesion molecule L1 is also involved in correct RGC projection along the posterior-to-anterior axis of the SC (Demyanenko et al., 2003). In L1-deficient mice, temporal axons projected ectopically to more posterior targets in the SC or IC (Demyanenko et al., 2003). It has been proposed that RGC axons need L1 to initiate the projection along the posterior-to-anterior axis of the SC by interacting with EphA/ephrinA signaling, although this possible interaction has not been described so far. The homeodomain transcription factor engrailed-2 (En-2) was shown

to have a dual function in the formation of the retinotectal projection in *Xenopus* and chicken. It is expressed in a caudal-to-rostral gradient in the tectum and its ectopical expression led to EphA ligand expression (Shigetani et al., 1997). Besides this gene-regulatory function, the transcription factor En-2 has a direct repulsive activity on *Xenopus* temporal axons while attracting axons originating from nasal retina *in vitro* (Brunet et al., 2005). All these observations suggest that there are more factors involved in retinal axon guidance displaying dual functions that are yet unknown.

Despite EphA/ephrinA forward signaling is likely not the only mechanism involved in R-C mapping it plays a major role in this process. In fact, on top of all genetic loss-of-function experiments described above, gain-of-function studies have demonstrated that this signaling is sufficient to direct retinal axons to specific locations in the colliculus. In chick, patches of exogenous ephrinA2 were produced in the embryonic tectum through infection with a retrovirus that contained ephrinA2. Via this manipulation, ephrinA2 patches were superimposed on endogenous ephrinA2 and -A5 randomly. Mid-temporal axons, which express high levels of EphA receptors and are sensitive to the membrane-associated chemorepellent of the C tectum, avoided the patches and mapped to R areas. In contrast, axons from nasal retina, which normally have a limited ability to distinguish between R and C tectal membranes, did not (Nakamoto et al., 1996).

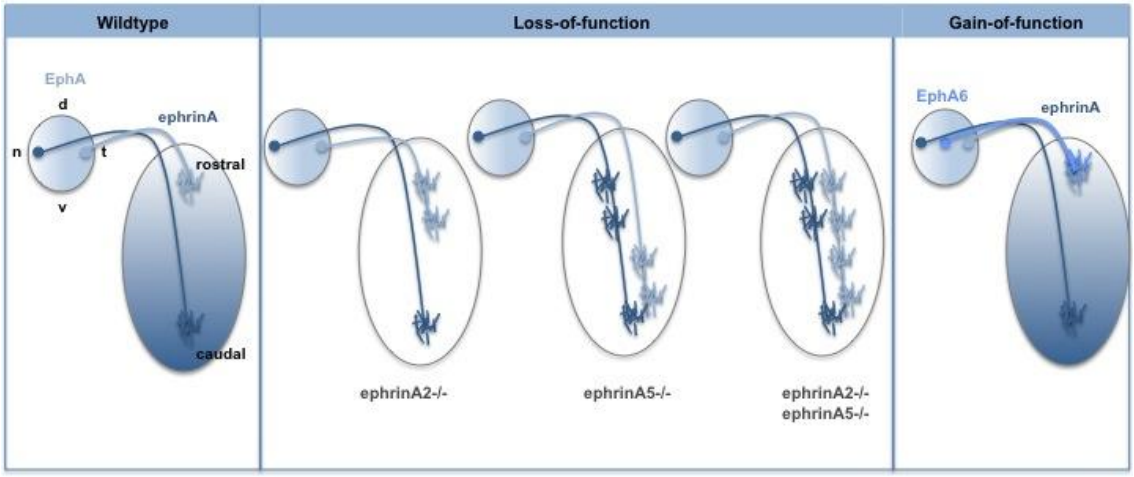

Figure 9. Mapping abnormalities in ephrinA mutant mice (LOF) and gain of function experiments (GOF). In ephrinA2 mutant mice temporal RGCs sometimes terminate in a second more caudal position at the SC whereas in ephrinA5 knockouts temporal RGCs also show mismapping, with a TZ in a more caudal area and nasal RGCs terminating in additional ectopic TZs. In double mutant mice multiple TZs are observed all along the R-C axis of the SC. GOF studies reveal that overexpression of EphA6 in the central retina is sufficient to send axons to the R area of the SC.

A more recent gain of function study used a gene knock-in strategy taking advantage of the facts that ephrinAs bind and activate most EphA receptors and that EphA3 is not expressed by RGCs in mice. In this study, EphA3 was ectopically expressed in about half of the RGCs in the mouse retina and this produced two subpopulations of RGCs, one with the WT gradient of EphA receptors (EphA5 and EphA6) and a second one with an elevated gradient of overall EphA expression resulting from the added expression of EphA3. In these mice, the projection of the EphA3 RGCs is compressed to the anterior half of the SC, indicating that the level of EphA receptor dominates the degree to which a RGC axon is repelled by ephrinAs. These results demonstrated that R-C topographic mapping is controlled by relative rather than absolute levels of EphA receptors in RGCs (Brown et al., 2000). Together with gain-of-function experiments performed in our laboratory in which EphA6 was overexpressed in RGCs from the center of the retina resulting in axons misprojecting into R areas of the SC (Carreres et al., 2011), all these observations demonstrate the

EphA/ephrinA signaling is sufficient to control most aspects of the R-C topographic mapping in the SC.

2.2.2 Spontaneous activity in retinocollicular map formation

Electrical activity is present from very early stages of development, way before the onset of sensory experience and synapse formation in the SC. This electrical activity that occurs before the beginning of sensory experience is known as spontaneous activity and has been described for all vertebrates (Wong, 1999). Accumulating evidence suggests that spontaneous activity might be important in early developmental stages such as differentiation, neural migration (De Marco et al., 2011), axon growth, axon guidance (Mire et al., 2012; Hanson and Landmesser, 2004) and map topography (Nicol et al., 2006; Nicol et al., 2007). It was not until Ca^{2+} was recognized as a second messenger and techniques for imaging appeared that fluctuations of intracellular Ca^{2+} were observed at early stages of neuronal development. The first recordings from embryonic retinas were obtained by Galli and Maffei in the rat retina (Galli and Maffei, 1988). Their studies demonstrated that neighboring RGCs become active in correlated bursts. After these findings, Meister et al., (1991) used multielectrode arrays and calcium imaging *in vitro* to show that RGCs and amacrine cells are activated in the form of waves that extend across certain areas in the retina during development. RGCs fire bursts of action potentials (AP) in the form of spontaneous waves (Shatz, 1996).

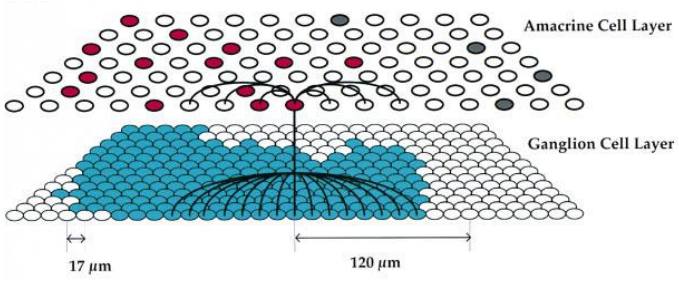

Figure 10. Model representing the generation of retinal waves. Each retinal ganglion or amacrine cell receives inputs from many other amacrine cells. When a high fraction of amacrine cells become active, a simulated wave will pass through those cells and be relayed to a contiguous distribution of ganglion cells. Spontaneously active amacrine cells not correlated with the wave are shown in gray (*Adapted from Feller et al., 1997).*

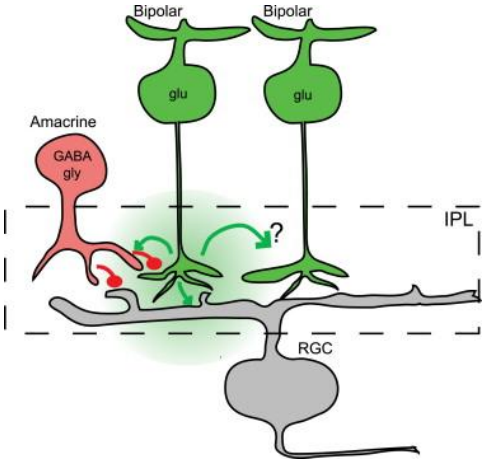

Figure 11. Changes in bursts of action potentials through the development of the retinal circuit. Wave propagation is mediated by excitatory connections that depolarize retinal ganglion cells. The circuit that mediates glutamatergic waves occurs between postnatal day 10 and 14, consists of bipolar cells, amacrine cells and retinal ganglion cells (*Adapted from Torborg and Feller, 2005).*

These waves are initiated at random locations by a class of cholinergic interneurons, the starburst amacrine cells, that spontaneously depolarize every approximately 15 seconds in the absence of synaptic inputs causing a large Ca^{2+} influx leading to the activation of neighboring RGCs (Huberman, 2008). Later, Feller et al., (1997) developed a dynamic model consisting on a coupled population of cells corresponding to the ganglion and amacrine cells that are involved in the neural circuit in charge of generating waves (Fig. 10). According to this model, amacrine cells are connected to each other, project to RGCs and can fire spontaneously. A wave would be initiated when a certain number of amacrine cells become active in a particular area of the retina. Retinal waves are considered to move slowly for a mechanism based on sequential synaptic activation of neighboring cells (50 – 200 µs). Spontaneous bursts of action potentials in the retina appear early in development and last until eye opening (postnatal day 13-14 in mice). These bursts of action potentials undergo several changes coinciding with the maturation of retinal circuitry (Fig. 11)

These changes can be divided in three stages; in the first stage waves depend on gap junctions and are present until P0 (Bansal et al., 2000). The second phase (the

most studied) lasts until P10. In this phase waves initiate in random locations and are propagated from starburst amacrine cells that release Acetylcholine (Ach) and depolarize neighboring cells (including RGCs). These waves can be blocked by Acetylcholine receptor (AchR) antagonists and persist in the presence of tetrodotoxin (TTX), which suggests that APs are not needed for the propagation of retinal waves (Stellwagen et al., 1999). The last stage (stage III) ranges from P10 to P14 and waves in this period are mediated by ionotropic glutamate receptors. The switch from Ach to glutamate is a gradual process and depends on the maturation of bipolar cells, the main glutamate source in the retina (Miller et al., 1999).

While the current assumption is that the activity patterns in the isolated retina reflect what occurs in the intact retina during development, no one has recorded retinal waves from a developing animal *in vivo* of any species so far. A recent study by Ackman et al., (2012) demonstrated that correlated spontaneous activity in the form of waves is present in alive neonatal mice by performing *in vivo* calcium imaging in both the SC and the visual cortex. The authors concluded that this form of activity propagates throughout the entire visual system before eye opening. However, these recordings were obtained from the SC and the visual cortex and not from the retina and therefore, for some authors, retinal waves might still be an epiphenomenon until it becomes possible to visualize them *in vivo* (Chalupa, 2009).

To start investigating the function of retinal waves, a few decades ago a group of researchers blocked retinal spontaneous activity by injecting TTX into the eye. These injections lead to a blocking of RGC APs that disrupted map refinement (O´Leary et al., 1986), revealing for the first time an important function of retinal activity in the formation of neural circuits. Genetic approaches in mice also showed that alterations in the cholinergic phase of retinal waves produce defects in axon refinement, particularly along the R-C axis (Chandasekaran et al., 2005). Mice lacking the β2 subunit of the nicotinic acetylcholine receptor (β2-/- mice) show no cholinergic

retinal waves during the first postnatal week and their RGCs exhibit an uncorrelated firing (Fig 12) (McLaughlin et al., 2003) that coincide with enlarged arborization in the SC (Fig 13) (Dhande et al., 2011). However, in these mice only cholinergic waves are affected and other forms of activity are still functional (Stafford et al., 2009) which could be masking an even more important function of spontaneous activity in this process. In addition, in these studies the authors do not specify whether the observed impairment in mapping is due to a defect in topography during the initial phase of the refining process or to later alterations in the local pruning and arborization at the TZ.

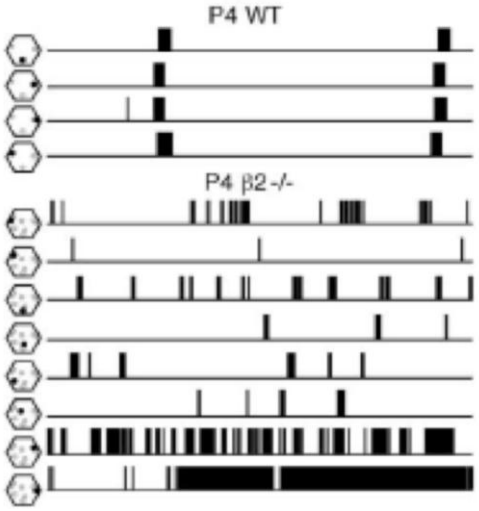

Figure 12. Mice lacking the β2 subunit of the nicotinic acetylcholine receptor show no retinal waves during the first postnatal week. Multielectrode recordings in a P4 retina show a lack of correlation between neurons in the β2 -/- retinas compared to the WT (*Adapted from McLaughlin et al., 2003).*

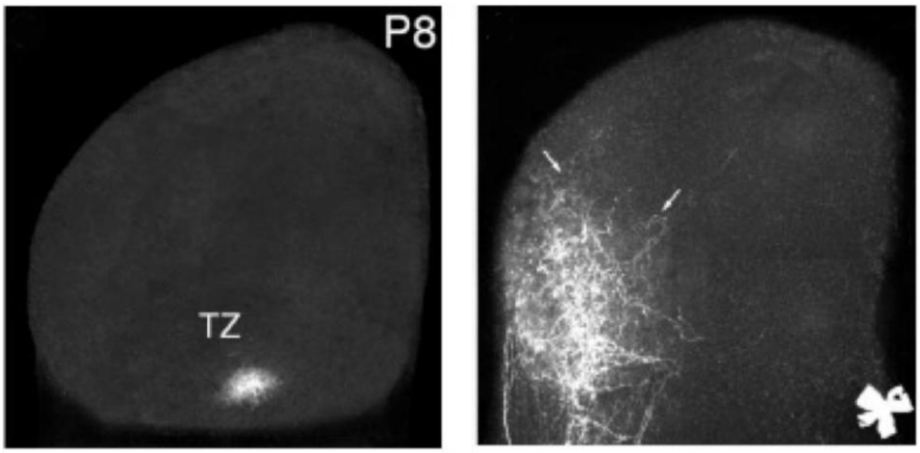

Figure 13. Altered retinal waves produce defects in axon refinement. On the left, normal TZ after large-scale remodeling, with axons projecting into the TZ at the topographically appropriate location in the SC. On the right β2-/- mice showing defective topographic remodeling of the retinocollicular projection *(Adapted from McLaughlin et al., 2003).*

It is clear however that blockade of spontaneous activity (correlated in waves or uncorrelated) alters circuit formation as shown in the above mentioned studies and as it was also elegantly demonstrated by a study in the visual system of zebrafish in which axon arbor growth was suppressed at the optic tectum after the blockage of spontaneous activity by ectopically expressing the rectifier potassium channel Kir2.1 in RGCs (Hua et al., 2005). However, given the reduced size of the zebrafish tectum compared to the large size of RGC arbors it was again difficult to distinguish whether spontaneous activity plays a role during the initial topography phase or later in arbor branching and pruning during the second phase of the maturation process.

2.2.3 Cross talk between spontaneous activity and Eph/Ephrin signaling

Few decades ago the prevalent hypothesis defended that in the visual system activity independent mechanisms generate a coarse topographic map relying on molecular cues, whereas the fine-tuning of this map required patterned neural activity.

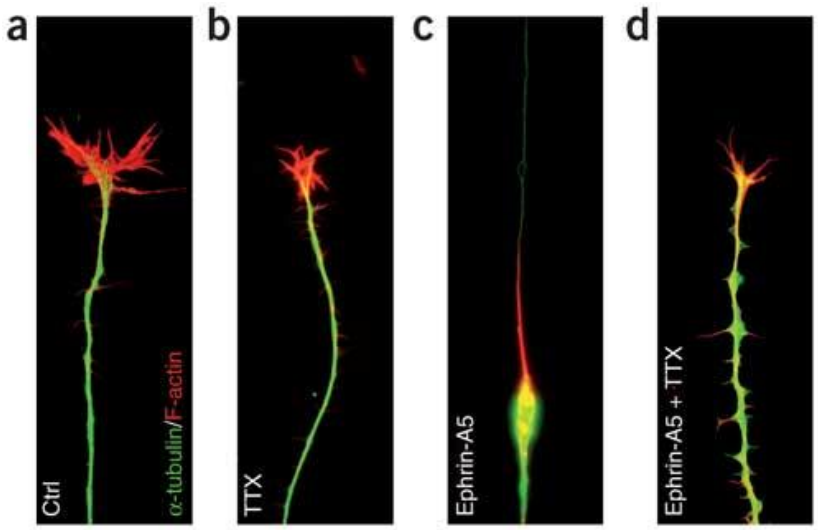

Figure 14. Blockade of calcium entry *in vitro* by TTX prevents the collapse of growth cones from temporal RGCs in response to ephrinA5. Axon collapse response was induced by bath applications of ephrinA5 on control E14.5 retinas grown on laminin-coated glass coverslips, and fixed 30 min later. (**a**) Typical retinal growth cone before drug application. (**b**) TTX does not alter retinal axon growth or growth cone morphology. (**c**) EphrinA5 induces a collapse with a long trailing process containing tubulin and an actin-rich retraction bulb. (**d**) TTX applied with ephrinA5 abolishes axon cone retraction but not lamellipodia collapse (*Adapted from Nicol et al., 2007).*

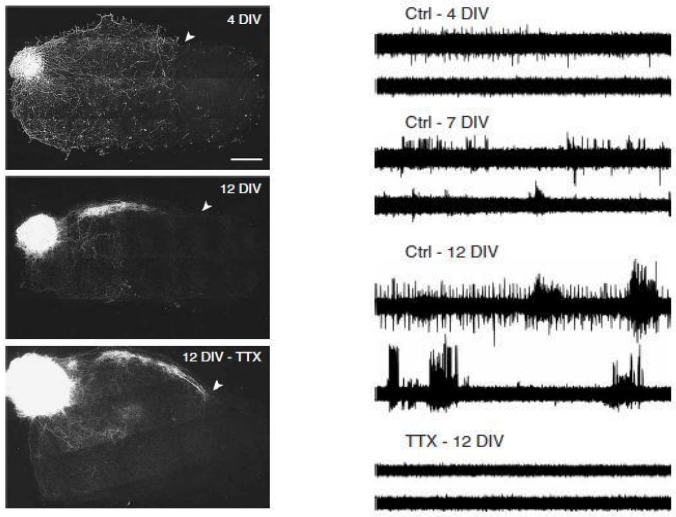

Figure 15. Spontaneous activity in the retina is required for the elimination of exuberant retinal axons in the SC *in vitro.* Organotypic retinocollicullar cocultures in which E15 retinas were confronted to P6 collicular explants and maintained up to 12 days in vitro in control medium or in medium supplemented with TTX. On the right, representative recordings from control and TTX treated cultures (*Adapted from Nicol et al., 2007*).

Although it is currently accepted that spontaneous neural activity plays a role in the refinement of visual circuits, there is an intense debate on whether it is exclusively permissive or has an instructive function. Furthermore, the exact contribution of the different types of waves described so far, is not clear yet (Huberman et al., 2008; Chalupa, 2009; Feller, 2009) and the molecular mechanisms by which spontaneous activity influences circuits´ wiring remain largely unknown. In this regard, the expression of certain classes of axon guidance molecules coincides with the moment of development in which spontaneous activity takes place, but it is still unknown whether or not molecular guidance cues and neural activity interact during development to finally generate the mature retinal projection patterns in the primary visual targets. Recent evidence *in vitro* appears to support the idea of an interaction between spontaneous activity and EphA/ephrinA signaling (Nicol et al., 2007). Nicol and collaborators showed that RGC axons coming from retinal temporal explants that express high levels of EphA responded to ephrinA5 by collapsing their growth cone. However, this collapse in response to ephrinA5 is abolished after calcium entry blockade by TTX (Fig. 14).

Nevertheless, these stunning results *in vitro* have not been replicated *in vivo*. So far, other experiments designed to address the putative relationship between spontaneous activity and EphA/ephrinA signaling *in vivo* in visual topography have produced unclear results. Mice lacking the acetylcholine nicotinic receptor crossed to ephrinA2/5 double KO mice show a nearly abolished retinotopic map in the visual targets (Cang et al., 2008; Pfeiffenberger et al., 2005), but this result was difficult to interpret, first because β2-/- mutants still retain correlated spontaneous activity in RGCs under specific circumstances (Stafford et al., 2009) and second, because the strong phenotype of ephrinA2/5 double KO mice cannot be assigned to the lack of ephrinA expression in the retina, in the SC or in both.

The relationship between spontaneous activity and EphA/ephinA signaling has been also suggested in other contexts. In the chick spinal cord, the expression of EphA receptors seems to change after the alteration of spontaneous activity patterns, which in turn affects motorneuron axon pathfinding (Hanson and Landmesser, 2004; Hanson and Landmesser, 2006; Hanson et al., 2008). However, although in these experiments spikes´ frequency was changed respecting to the wildtype situation, activity was not abolished and therefore it is not clear whether in this context, spontaneous activity is required for EphA expression or for activation of the EphA/ephrinA signaling. Also related to possible interactions between guidance molecules and spontaneous activity, recent data on the development of thalamocortical circuits have suggested a role for spontaneous activity in the transcriptional regulation of guidance receptors such as Robos (Mire et al., 2012).

In summary, along the last few decades it has become clear that neural circuits in the mammalian brain develop through a combination of axon guidance molecules and activity-dependent refinement mechanisms. However, the relative contribution of each of these factors remains undefined. The possibility of a relationship between guidance molecules and spontaneous activity has become one of the most controversial issues for researchers studying neural development and experiments using the visual system as a model have opened an intense debate defending an interaction between EphA/ephrinA signaling and spontaneous activity during the refinement of topographic visual maps. In addition, increasing evidence from other systems now suggest that spontaneous activity might be essential for early developmental stages such as differentiation, axon growth and guidance.

AIMS

AIMS

- To investigate the existence of retinal waves *in vivo* as previously described by *in vitro* studies.
- To develop genetic tools to permanently block spontaneous activity in retinal ganglion cells *in vivo* and analyze its function during early stages of visual development.
- To clarify the controversial question of whether retinal spontaneous activity is required for the activation of the EphA/ephrinA signaling during retinocollicular map formation *in vivo* and define the specific roles of EphA-ephrinA signaling and spontaneous activity in the formation of the rostrocaudal retinocolicular map.

MATERIALS AND METHODS

1. Optic fiber calcium recordings *in vivo*

1.1 *Animals*

ICR postnatal mice were obtained from a breeding colony at the Barrow Neurological Institute.

The FCM1000's fibered microprobe (Fig. 16) is designed to reach virtually anywhere inside a living animal allowing high-speed recordings of cellular or vascular events by simply contacting the tissue of interest, in our case the retina of neonatal mice. With the FCM1000 fibered micro-endoscope we have obtained real-time (12 f/s) *in vivo* calcium retinal recordings in neonatal mice with cellular resolution, minimal invasive fashion and minimal disturbance of the process under investigation. This technique allows the isolation of calcium transients in the developing retina *in vivo* between P5 and P12, before eye opening.

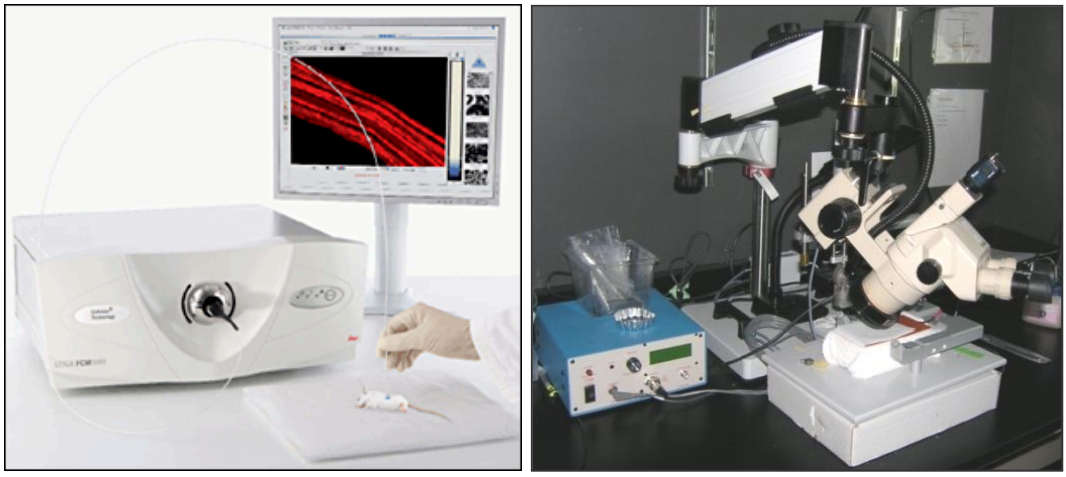

Figure 16. Microscope used for surgery and optic fiberscope used for *in vivo* recordings. On the left, FCM1000's fibered microprobe used for *in vivo* recordings. On the right, Cellvizio microscope used for surgeries and for visualizing fiber insertion.

1.2 General surgical methods

Surgeries related to the The FCM1000 fibered micro-endoscope were performed under aseptic conditions. P5-P12 Mice were anesthetized with ketamine/xylazine or isoflurane (100 mg/kg / 10 mg/kg or 3% in the case of isoflurane). The level of anaesthesia was carefully monitored and redosing was administrated when needed (one-third to one-half of the original dose). Body temperature was controlled and continuously monitored with a heating blanket set to 37°C. Temperature inside the eye was also monitored using a Physitemp (BAT-12) inserted into the contralateral eye of the mouse. Animals were attached with adhesive tape to a plastic surface placed on an electric blanket used to maintain body temperature constant (37º).

The fibre-optic objective was attached to a Cellvizio microscope (Leica FCM-1000, Leica Microsystems, USA) and introduced into the eye after separating both the conjunctiva and the eyelid of the animal. A computer controlled robotic microdrive (StereoDrive, Neurostar, Germany) was used to ensure equivalent placement in all animals. The robotic micromanipulator arm anchored the fibre-optic probe from above so that the probe entered the eye and reached the retina accurately (Fig. 17).

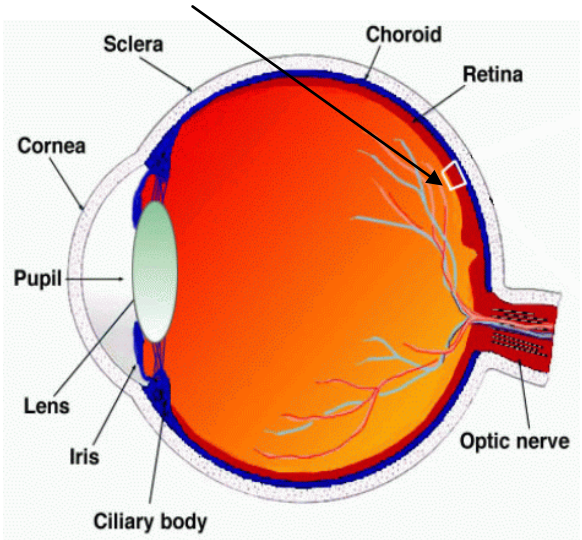

Figure 17. Schematic representation of microprobe retinal insertion. Arrow indicates the trajectory of microprobe insertion into the retina.

Before recordings, all animals were eye injected with the Fluo4 calcium marker (Invitrogen, USA) and placed on the heating blanket for an incubation period of 2 hours. After each recording session, each animal was deeply anesthetized with Nembutal and sacrificed (100 mg/kg). In some cases the retina was extracted and placed in a Petri dish with an extracellular solution containing (in mM) 135 NaCl, 5 KCL, 2 CaCl2, 1 MgCl2, 10 HEPES and 10 Glucose used to keep the tissue alive. Immediately after extraction retinas were mounted on glass slides and fluorescence imaging was used to identify Fluo4 loaded cells and fibre insertion area (Fig. 18).

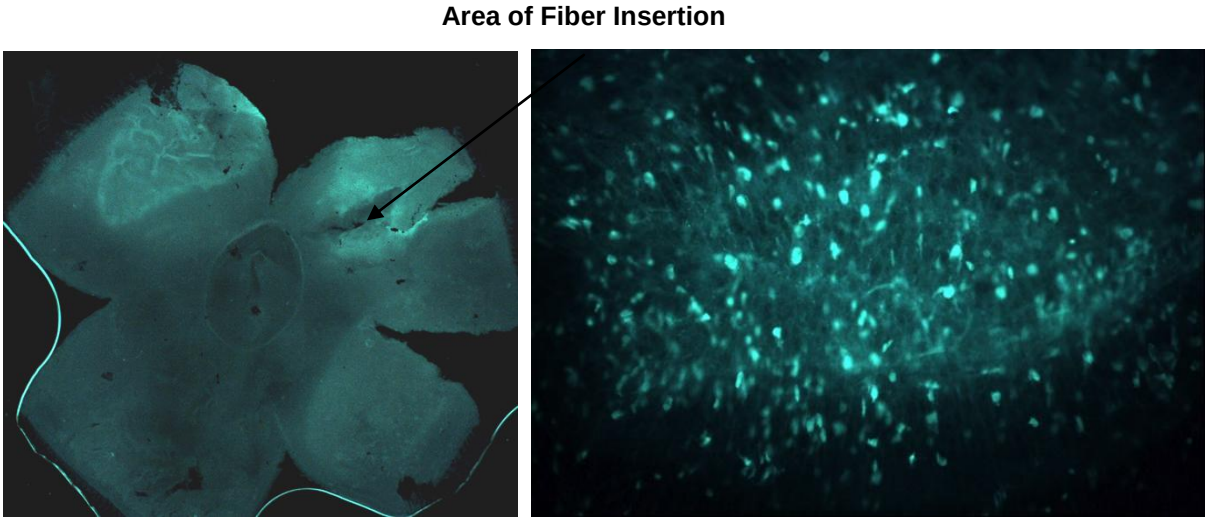

Figure 18. Retinal extraction after *in vivo* calcium recordings. On the left, fibre insertion mark. On the right, Fluo4 loaded cells.

1.3 Fiber-coupled confocal image analysis

A blind analyst measured calcium transients and waves´ dynamics automatically and objectively via custom MATLAB software. The same method analysis as in Blankenship and Feller (2009) was used for transient analysis. We used a spatial filter of 31 x 31 µ and a grid of 5 x 5 points, measuring the interwave interval passing through that area. Different area sizes were used (covering just 80% of the area instead of 100%) to not miss any calcium wave.

For calcium transient detection, data was initially detrended (high-pass filtered) and smoothed with a Savitzky-Golay filter. Two different thresholds were used

for the analysis. First, two consecutive samples of the derivative higher than 2 SDs from the mean of the derivative of the whole recording defined the starting point of a given transient. Second, within the first two seconds, fluorescence amplitude should reach a level above two SDs of the whole recording. For calculating correlations between all the ROIs we calculated the distances and the scaled cross correlations pairwise. To do the averages, we divided all the distances in different percentiles in order to have the same number of correlations to average in all the traces.

2. Electroporation *in utero*

2.1 *Animals*

ICR mice obtained from a timed pregnancy-breeding colony at the Instituto de Neurociencias de Alicante were used in all the experiments. E0 was defined as midnight of the night before a plug was found.

2.2 General surgical methods

Pregnant ICR females were anesthetized with isoflurane (5% for induction, 2% during surgery, Harvard Apparatus) and attached with adhesive tape to a plastic surface placed on an electric blanket used to maintain body temperature constant (37º). This immobilization facilitated mice rotation and improved DNA injection into embryo´s eyes. In order to avoid abortion and uterus opacity 0.15 ml ritodrine (Sigma) was injected intraperitoneally before the surgery (0.1 ml of a 14 mg/ml solution). Buprex was injected subcutaneously (3µl/g) to minimize post-surgical pain. After cleaning the abdomen with 70% ethanol a 3-cm midline laprotomy was performed and the uterine horns exposed.

2.3 *In utero* electroporation

For DNA microinjection, 68-mm graduated pulled glass mouth-micropipettes (World Precission Instruments, Inc.) were pulled by using a micropipette puller P-2000 (Sutter

Instruments) to a tip of less than 20 microns. EGFP expressing plasmids were injected monocularly through the uterus wall into each embryo using a mouth controlled pipette system (Drummond scientific) and a Leica KL 1500 LCD lamp. We found it more convenient to use a graduated mouth-micropipette than a picospritzer because it facilitated the rotation of the mother when access to the embryo's eye was restricted (Fig. 19).

DNA solutions were used as follows depending on the experimental condition: for the EGFP and EphA6 controls 1µg/µl plasmid was used. For the Kir2.1 condition 1.5µg/µl CAG-Kir2.1 was used and for the combined EphA6 and Kir2.1 condition both plasmids were mixed (1.5µg/µl CAG-Kir2.1 and 1µg/µl EphA6, respectively). In those cases used for axonal reconstruction the concentration of CAG-EGFP plasmid was diluted to 0.2ug/ul and CAG-Kir2.1 was 0.5ug/ul and the electroporation was performed at E16 to diminish the number of targeted RGCs. All plasmids were diluted in a solution containing 0.03% Fast Green in TE in order to visualize the injected solution.

The head of each embryo was placed between tweezer type electrodes (CUY 650-P5 Nepa GENE, Chiba, Japan) consisting on a pair of platinum round plates with a 1cm diameter (Fig. 20). Five squares electric pulses (50ms) were delivered at 950 ms intervals using an electroporator (Square wave electroporator CUY21SC, Nepa GENE). The uterus was kept wet by dropping saline (prewarmed at 37°C) between the electrodes. EGFP expression was only detected in retinal cells of embryos electroporated with the positive electrode placed on the injected eye (Fig. 20), indicating that DNA is transduced from the sclera side, where undifferentiated and newly post-mitotic cells are located. About 70% of the embryos expressed GFP in the retina and no damage was evident in the electroporated retinas, as previously described in Garcia-Frigola et al. (2007). Voltage conditions depended on the developmental stage of the embryo. For E13.5 embryos 35 V pulses were applied. Optimal voltages for each age are further described in Table 1. After embryo

electroporation the abdominal cavity was sutured closed and the pregnant female was placed in a 37º chamber in order to recover from anesthesia. Embryos were allowed to develop normally until the day of birth (P0) or until P9.

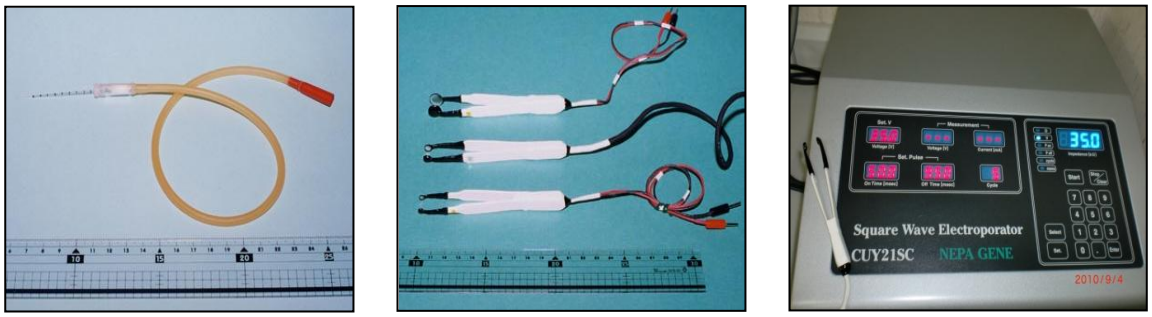

Figure 19. Mouth controlled pipette system, paddle electrodes and electroporator. *(Adapted from Saito and Nakatsuji 2001).*

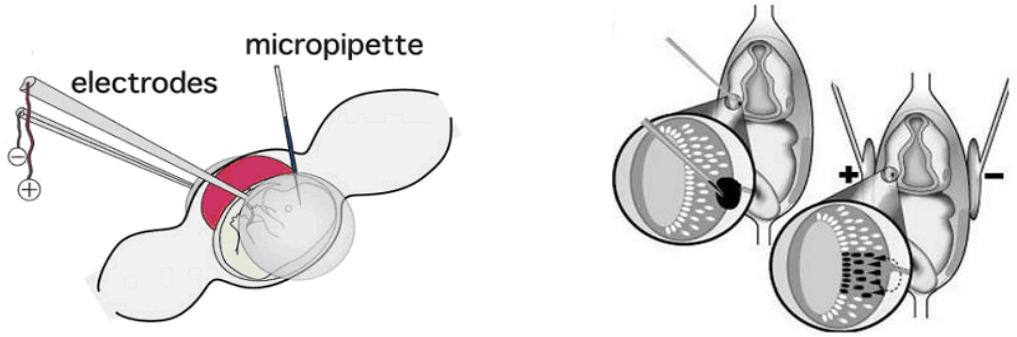

Figure 20. Schematic representation of a micropipette and electrodes. Paddle electrodes are placed on the uterine wall to pass the electric pulses after DNA injection with a micropipette. The positive electrode is located on the injected eye and the negative on the opposite side *(Garcia-Frigola et al., 2007)*

Conditions for Electroporation at Different Stages and Survival rate

Embryonic stage	Pulses (ms)	Voltage (V)	DNA Concentration (ug/ul)	Survival at P9 (%)
E13. 5	50x5	35	Kir2.1 (1.5); EphA6 (1); EGFP (0.5)	40
E16.5	50x5	40	Kir2.1 (1); EphA6 (0.8); EGFP (0.3)	55

Table 1. Optimal conditions for electroporation at different embryonic stages. Summary of pulses, voltage and DNA concentrations used in our experiments and survival rate of embryos electroporated at two different stages.

3. Immunohistochemistry.

Serial floating SC vibratome sections (80 µm) or wholemount retinas were immunostained with the following primary antibodies: rabbit anti GFP (1:2000, AbCam), rabbit anti Kir2.1 (1:800, AbCam), rabbit anti Caspase-3 (1:500, Cell signaling). The following secondary antibodies were used: Alexa Fluor 488 goat anti rabbit, Alexa Fluor 594 donkey anti rabbit and Alexa Fluor 633 goat anti rabbit. Sections and wholemount retinas were washed five times during 10 minutes with PBS-T (PBS 1X mixed with 0.1% Triton 100x) and then incubated for 2 hours at room temperature with a blocking solution containing 1% BSA, PBS-T and 10% horse serum.

Blocking solution was removed and brain sections incubated with the primary antibody overnight. Primary antibodies were then removed and all slices were rinsed out four times during 10 minutes each with PBS-T and further incubated with the coupled secondary antibody for at least 1 hour. Antibody incubation was followed by four washings of 10 minutes each with PBS-T followed by Dapi staining (1:1000 in PBS 1X) to visualize cell nuclei. All immunostained slices were mounted on glass slides and coverslipped with Fluoromount (Sigma).

4. Two photon and confocal imaging

Two photon and confocal imaging were used to perform calcium imaging in order to demonstrate that RGCs electroporated with Kir2.1 showed no neural activity. For that purpose mice were electroporated with the fluorescent marker DsRed instead of GFP in order to distinguish the electroporated cells (in red) from those loaded with the calcium marker Fluo4 (in green). Retinas from embryos electroporated with CAG-DsRed and CAG-Kir2.1 plasmids were bulk loaded with the calcium indicator Fluo4 (Invitrogen) using a variant of the multicell bolus loading technique (Stosiek et al., 2003). Fluo4 solution was injected into the vitreous chamber of anesthetized mice with a micropipette. Up to 4 injections were applied to each animal. Mice were placed on a

warm surface set at 37º for an incubation period of 2 hours after which they were anesthetized for decapitation and retinal extraction. This incubation method *in vivo* allowed us to assure the viability of RGCs avoiding cell damage and/or death. After dissection (using a Leica MZ FLIII) retinas were placed in a petri dish with ringer solution containing (in mM) 135 NaCl, 5 KCL, 2 CaCl2, 1 MgCl2, 10 HEPES and 10 Glucose and mounted with the RGC layer side-up on a cellulose nitrate membrane (Whatman). The membrane was then placed on the top of a filter connected to a 50ml syringe and vacuum was performed to extend the retina and have direct access to the RGC layer. Fluorescence imaging was used to identify the electroporated RGCs and pictures of the electroporated area were taken. Epifluorescent calcium imaging was performed using a DM LFSA microscope (Spectra Physics, Neslab KMC 100) using a 10x or 20x water immersion objective with illumination provided by a Leica TCS RS (Fig. 21). The nitrocellulose membrane was fixed to the base of the petri dish for avoiding motion artifacts during the recordings. Calcium transients were recorded in 3 minutes´ epochs. Due to tissue bleaching in two photon recordings only those experiments performed in confocal mode were used for quantification.

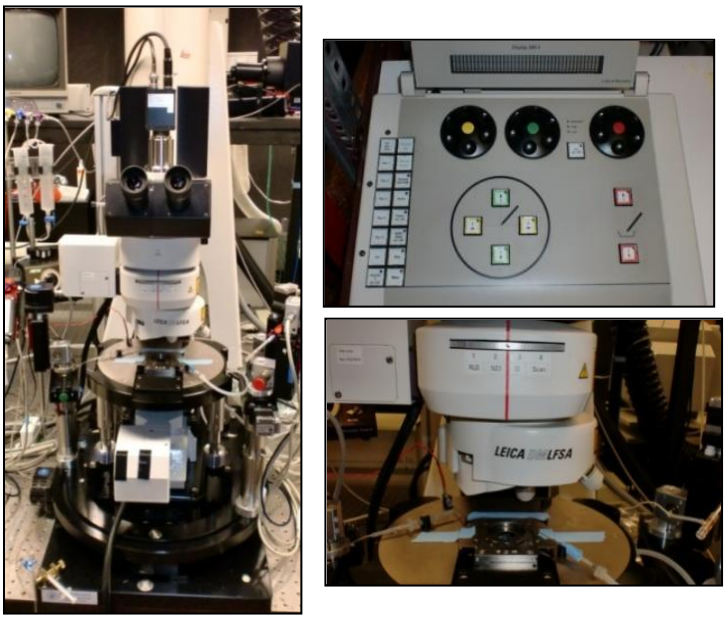

Figure 21. Microscope and micromanipulator used for calcium recordings. On the left image of the microscope (DM LFSA) used to perform calcium imaging in the retina. On the right micromanipulator and below closed-up image of the microscope with the different objectives.

5. Histology

After fixation by cardiac perfusion with 4% paraformaldehyde in PBS, electroporated retinas and SCs of P0 and P9 mice were photographed with fluorescence optics as whole mounts. Prior to retinal removal cuts were made in the retina to maintain orientation. SC size was determined by measuring the distance along the rostral-caudal axis from the rostral border of the SC to the most distant point along its caudal edge. Some colliculi of each age group (P0 and P9 respectively) were embedded in 3% agar and sectioned sagitally at 80 µm on a vibratome (Leica VT 1000 S). Each section was mounted serially on glass slides, examined under fluorescence and photographed.

5.1 Histological imaging

Histological SC and RGC images were obtained using a Laser Scanning Confocal Microscope Leica TCS SP2 AOBS (Leica Microsystems). Images (1024 x 1024, speed 400 Hz) were taken using three different objectives: HC PL APO CS10x objective n.a 0.4 dry, HC PL APO CS 20x objective n.a 0.7 dry and HCX PL APO lbd BL 63x objective n.a 1.4 oil. Two different channel settings were used for the pictures: GFP (spectral detector range 500 – 550 nm) and Alexa 594 (spectral detector range 590 – 710 nm).

6. Analysis of targeted axons at the SC

Despite the fact that the use of *in utero* electroporation is a very powerful technique for functional developmental *in vivo* studies it conveys some limitations such as the unfeasibility to quantify the number of targeted RGCs. To reduce variability in our analysis we used those retinas electroporated in equivalent central areas and to better analize topography and branching we introduced low concentrations of DNA in order to target and visualize single cell axons. We conformed three reconstructed serial sections from each animal to a single common template of the SC (Fig. 22). The common template represents a sagital slice cut through the centre of the SC at a

medio-lateral coordinate where the dorsal layer is relatively homogeneous and flat. The common template was chosen in a way that minimizes the mean square distortion arising from piecewise-linear conformation of tissue sections from individual animals to this template. To do so, we first linearly scaled all sections to the mean thickness of the dorsal layer of the SC. We then measured fluorescence levels along the rostrocaudal axis of the SC, divided in 124 homogeneous bins to gauge the spatial distribution of the terminal arbours of different populations of RGC axons. We used a bin-by-bin ANOVA-one way test to quantify the differences between the distributions of fluorescence intensity.

Figure 22. Example of analysis of targeted axons at the SC. On the left, a retina electroporated with EGFP in central area. Only embryos with retina electroporated in an area similar to the one shown in the figure were used to analyze the corresponding SC. On the right, common template used for analyzing fluorescence intensity in the SC of a P9 mice

7. qRT-PCR

qRT-PCR for EphA6 and ephrinA5 was performed using the same protocol and primers than previously described (Carreres et al., 2011). Retinas of E13.5 wild-type embryos were electroporated *in utero* with CAG-GFP alone or together with CAG-Kir2.1 plasmids. Embryos were allowed to develop for 3 days and then their retinas were removed. Each electroporated retina was observed under a fluorescence microscope and the electroporated GFP-positive retinas were dissected out and kept for RNA

extraction. Ten retinas were used for each experiment. Total RNA was extracted using the RNeasy Mini Kit (Qiagen), DNaseI digested and retrotranscribed using the Reverse Transcription System (Promega) the following manufacturer's recommendations. Quantitative (q) PCR was performed using an ABI PRISM 7000 sequence detection system with the SYBR Green method. Primers were designed using Primer Express (software v2.0, Applied Biosystems): To detect Kir2.1 the following primers were used: Fw: AACCAACCGCTACAGCATCGT;Rv: TTCTTCACAAAGCGGCTCCTG. Transcript levels were calculated using the comparative Ct method normalized to Gapdh's (levels). The final results were expressed relative to calibrator (control embryos electroporated with CAG-GFP) using the $2^{-(\Delta\Delta Ct)}$ ± s.e.m. formula.

8. Axon arbor reconstruction in single cell electroporation

Confocal microscopy using Leica Confocal Software TCS SL (Leica Microsystems) was used for collecting Z stacks from P9 SC previously stained for GFP as described in the immunohistochemistry section. Images (1024 x 1024, speed 400 Hz) were taken using two different objectives: HCX PL APO CS 20x objective n.a 0.7 dry and the HCX PL APO CS 40x objective n.a 1.25 oil). Maximum projections were used for 3D axon arbor reconstructions obtained with Imaris Scientific software (Bitplane AG) and "movies" were created with a rotation angle of 360º.

Quantification of axon arborization was performed with ImageJ using the polygon tool for ROI section to measure width and percentage of area covered by axonal projections (measured as fluorescence intensity or I). Moreover, distance to surface was measured using the "straight" tool, taking the axon tip that was closest to the SC surface as a reference point and measuring from there to the SC surface.

RESULTS

1. Correlated firing of RGCs *in vivo*.

In the last few years, an enormous relevance has been attributed to patterned retinal spontaneous activity in the form of waves during the formation of visual circuits. However, at the point of starting this thesis there were no evidences of retinal waves *in vivo*. Therefore, we wanted to investigate whether retinal waves are a physiological phenomenon and, in order to analyze the presence of retinal calcium waves *in vivo,* we used optic fiber microscopy to perform calcium imaging in WT mice ranging from P5 to P10 (Fig. 23).

For these experiments, we injected the calcium marker (Fluo4) into the eye of the anesthesized animal (with either Ketamine or Isoflurane) and waited for an incubation period of 2 hours, after which we performed a surgery that allowed us to insert the fiberscope into the animal´s eye while keeping the body and the eye temperature constant (at 37º and 32º, respectively). Recordings were performed for a minimum of 3 minutes and a maximum of 6, after we managed to control for both bleaching and motion artifacts derived from breathing difficulties and/or anesthesia readministration. After data analysis we observed the presence of calcium transients occurring with an average duration of 2.6 $^{+}$/- 1.7 seconds and with an average magnitude of 8.5 $^{+}$/- 2.9 df/f (Fig. 24)**.** Percentage of recordings with transients was 75.9%. Average onset rate was 0.3 +/- 0.1 transients/minute (N=15 retinas)**.**

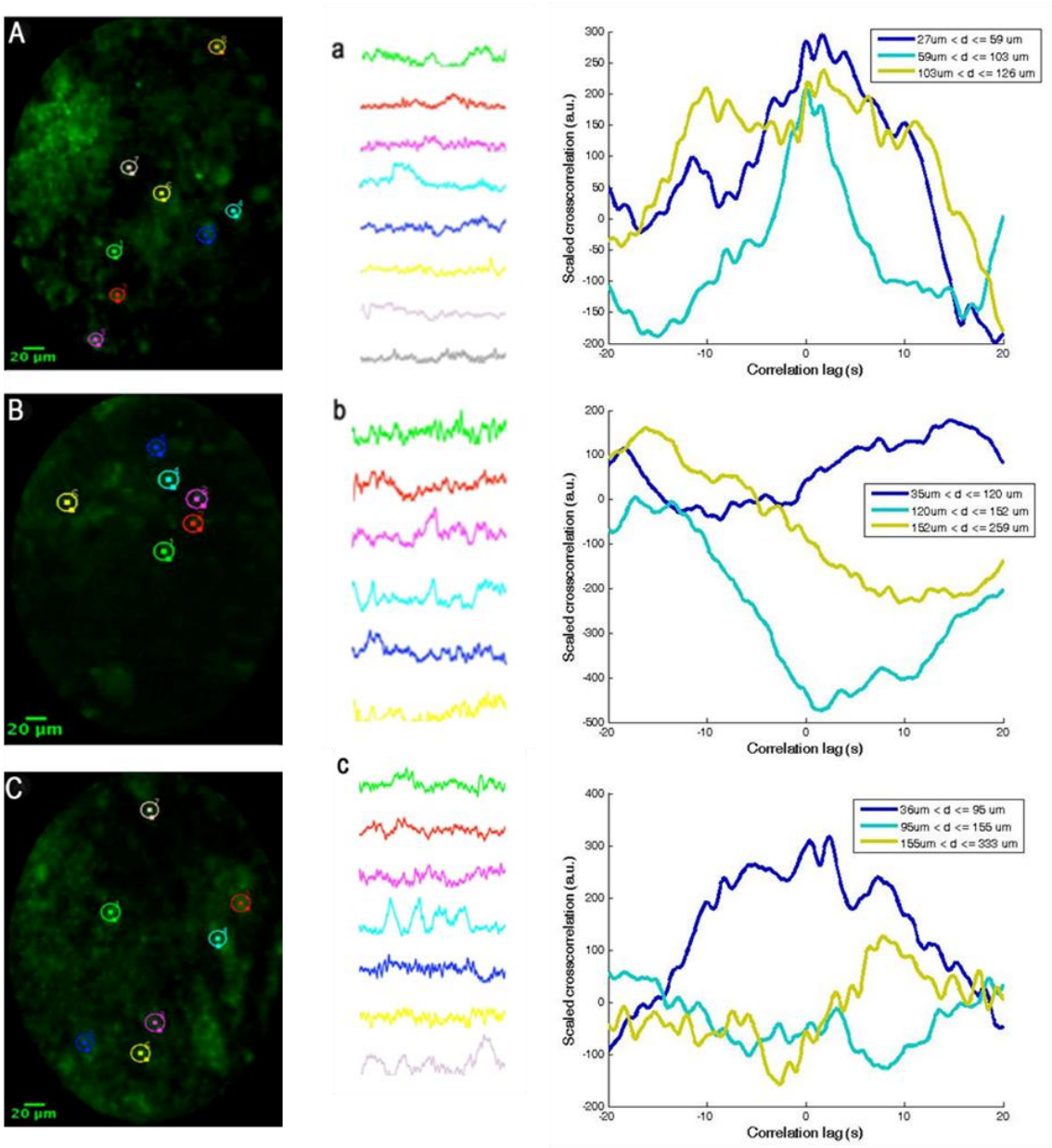

Figure 23. Raw data showing calcium imaging in different retinas. A, B and C represent retinal recordings from a P8, P9 and P11 retina, respectively. a, b and c correspond to transients isolated from ROIs in A, B and C. Right graphs represent raw correlations between different ROIs showing that pairwise fluorescence measurements of RGCs placed close to each other in the retina present higher correlations.

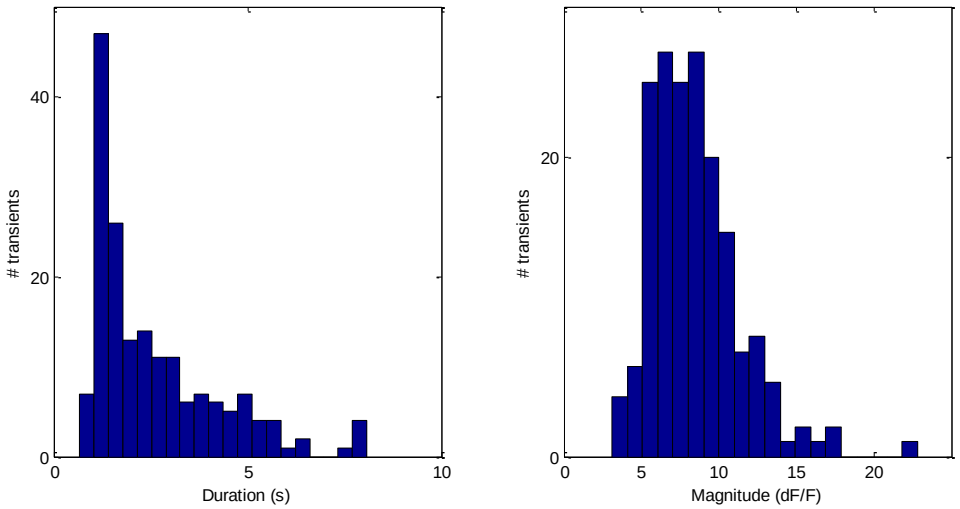

Figure 24. Statistics representing duration and magnitude of retinal calcium transients. On the left graph showing average transient duration from all recordings. On the right average of transients´ magnitude is represented.

We found a clear correlation between RGCs that were located close to each other in the retina (Fig. 25). Therefore, our results are in line with previous findings obtained by Galli and Maffei (1988), describing a correlation between neighboring RGC in the rat retina. Due to the low spatial resolution of these pioneering experiments the authors did not describe the presence of any retinal waves but defended a correlation in firing patterns between neighboring cells. Our results are in agreement with these previous *in vivo* results showing early correlated activity of RGCs, but as them, we have not been able to isolate the same retinal wave patterns as the ones described by *in vitro* experiments even in more mature stages than those from Galli and Maffei studies.

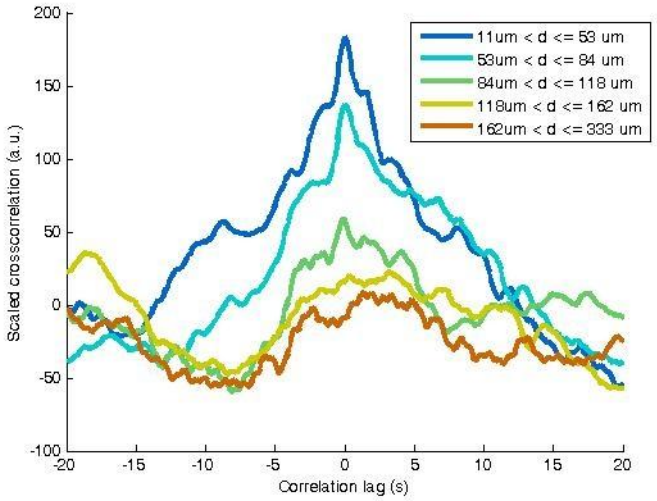

Figure 25. Correlation between RGCs placed near to each other in the retina. Graphs plotting average correlation from pairwise fluorescence measurements from all animals showing that correlation between different ROIs decreases with distance.

2. Blockade of spontaneous activity in RGCs *in vivo*.

In order to precisely study the influence of spontaneous activity during the development of visual maps we have developed an approach to block the activity of RGCs from embryonic stages *in vivo*. We have ectopically expressed Kir2.1 (an inward rectifying potasium channel) in RGCs by using *in utero* electroporation. Inward rectifying potassium channels are a specific subset of potassium channels and can be divided in seven subfamilies. Inward rectification of potassium permeability refers to increases of potassium conductance under hyperpolarization and decreases under depolarization, the opposite effect to that of outward or delayed rectification that is seen in voltage gated potassium channels. This current has a role in regulating neuronal activity helping to establish the resting membrane potential of the cell (Lopatin and Nichols, 1997). Particularly, ectopic expression of Kir2.1 has been succesfully used to block neuronal activity in a number of different cell types and tissues (Burrone et al., 2002; De Marco et al., 2011; Yamada et al., 2010; Mire et al., 2012).

Our laboratory has shown that, *in utero* electroporation after introduction of plasmids into E13 embryos, results in the targeting of a considerable amount of differentiating RGCs (Garcia- Frigola et al., 2007). Therefore, we used this approach and this developmental stage to deliver plasmids containing Kir2.1 in the embryonic retina to specifically block activity in RGCs. The coding sequence of Kir2.1 driven by a general promoter CAG (a very strong and ubiquitous promoter that contains a modified chicken β-actin promoter with a cytomegalovirus-immediate early enhancer) (CAG-Kir2.1) was introduced in E13 retinas by *in utero* electroporation together with plasmids containing the coding sequence of the fluorescent protein EGFP (CAG-EGFP) (see Materials and Methods). We coelectroporated CAG-EGFP and CAG-Kir2.1 plasmids instead of using bicistronic constructs (CAG-Kir2.1iresEGFP) because ires-EGFP leads to very low levels of EGFP, which complicates axons visualization. Electroporated animals developed normally and their retinas were analyzed at different stages between P0 and P9. First, we tested if Kir2.1 and EGFP are coexpressed in RGCs after electroporation. For this, wholemount retinas from P0 and P9 animals co-electroporated with CAG-Kir2.1 and CAG-EGFP were incubated overnight with anti-GFP and anti-Kir2.1 antibodies. Using confocal microscopy, we observed that targeted RGCs were positive for both EGFP and Kir2.1 in almost 100% of the cases (Fig. 26). Therefore, co-electroporation of two plasmids (one of them coding for a reporter protein) is a good method to visualize the cells ectopically expressing the gene of interest.

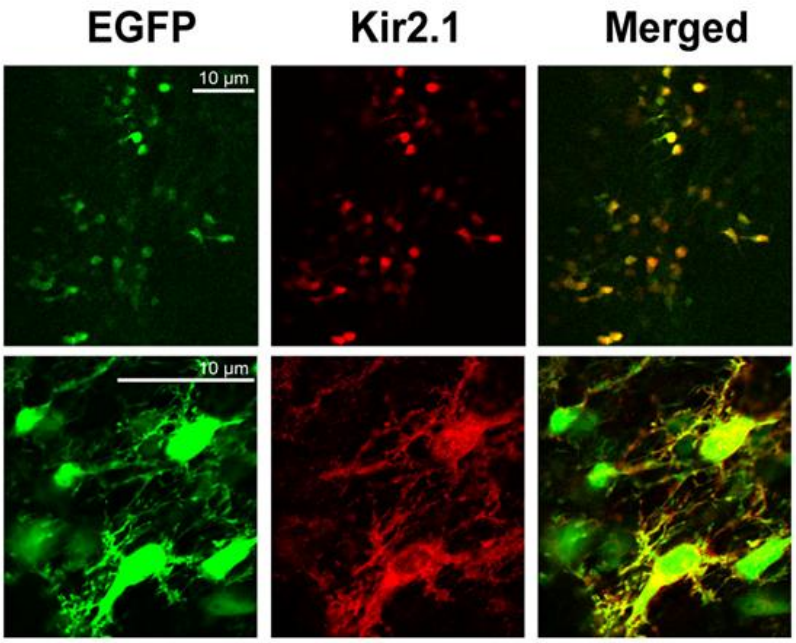

Figure 26. Coexpression of Kir2.1 and EGFP in RGCs. Plasmids bearing the coding sequence of Kir2.1 plus EGFP were injected into the embryonic retina of E13 embryos by *in utero* electroporation. Retinas from electroporated mice were dissected at P9 for immunohistochemistry, performed in flattened wholemount retinas. Bottom panels show higher magnifications.

To analyze if ectopic expression of Kir2.1 blocks spontaneous activity we performed two-photon calcium imaging in wholemount retinas electroporated with CAG-Kir2.1. Retinas co-electroporated with CAG-Kir2.1 and CAG-DsRed were loaded with the calcium marker Fluo4. For these experiments we coelectroporated Kir2.1 with DsRed instead of with EGFP because Fluo4 presents a wavelength similar to that of EGFP (Fluo4 shows an excitation peak at 485 nm and an emission peak at 520 nm whereas EGFP presents an excitation peak at 488 nm, with an emission peak of 509 nm). We performed 3 minutes movie recordings in each electroporated area. This duration was determined following previous literature describing the temporal detection of calcium transients (Torborg and Feller, 2005). Average measure of the total calcium spikes per minute in RGCs expressing Kir2.1/DsRed revealed a complete absence of calcium transients, contrary to what we observed in neighbouring non electroporated

RGCs. Quantification was performed using 56 cells from 5 animals electroporated with DsRed/Kir2.1 (Fig. 27). These experiments demonstrate that we can use Kir2.1 *in vivo* to permanently block calcium transients in a restricted population of RGCs.

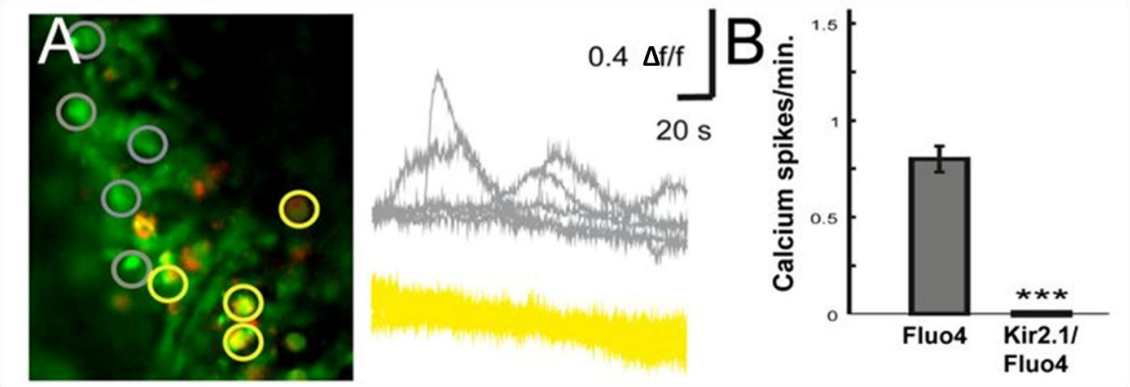

Figure 27. Ectopic expression of Kir2.1 blocks calcium transients in retinal ganglion cells. A. Grey ROIs represent cells loaded with Fluo4 (not electroporated cells) and yellow ROIs cells electroporated with Kir2.1/DsRed and loaded with Fluo4. Waveforms show examples of calcium activity taken from each ROI. **B.** Absence of calcium transients in Kir2.1 electroporated RGCs and normal pattern of spontaneous calcium activity in the Fluo4 control cells. ***p<0.001. Error bars represent ± s.e.m. Student´s unpaired test.

3. Differentiation, axon growth or pathfinding are not altered after RGC activity blockade

Different lines of evidence have suggested that spontaneous neuronal activity maybe essential for cell survival, specification, cell migration, axon guidance or pathfinding at early developmental stages (De Marco Garcia et al., 2011; Goodman and Shatz, 1993; Uesaka et al., 2005; Cohan and Kater, 1986; Kastanenka and Landmesser, 2010; Hanson and Landmesser, 2004; Hanson et al., 2008). To date, retinal spontaneous activity has been blocked in postnatal animals but the effect of activity blockade in embryonic stages has not been previously tested in the developing visual system.

It has been described that apoptosis of the RGC cell body is mediated by the activation of the caspase-3-dependent system (Nikolaev et al., 2009). To investigate whether activity inhibition at early embryonic stages affects survival of RGCs we first

checked for apoptosis in RGCs after electroporation of Kir2.1 at E13. Coronal sections from P0 and P9 animals electroporated with CAG-Kir2.1 and CAG-EGFP plasmids were incubated overnight with anti-Caspase3 antibodies (N = 3). Sections of the olfactory bulb were used as positive control because at this stage this area shows a high rate of cell death (Holcomb et al., 1995; Cowan et al., 2001; Cowan and Roskams, 2004). Consistent with previous results, we observed many cells positive for Caspase-3 in the olfactory bulb but this number did not increase in RGCs ectopically expressing Kir2.1 compared to not electroporated adjacent retinal neurons (Fig. 28).

Thus, ectopic expression of Kir2.1 in RGCs during development does not produce any cell death. To analyze the requirement of spontaneous activity for axon growth and guidance we examined the optic chiasms of E16 embryos electroporated at E13 with CAG-Kir2.1/EGFP or CAG-EGFP alone. At the optic chiasm level, axons from RGCs ectopically expressing Kir2.1 behaved similar to control axons electroporated with CAG-EGFP alone (n=7) (Fig. 29).

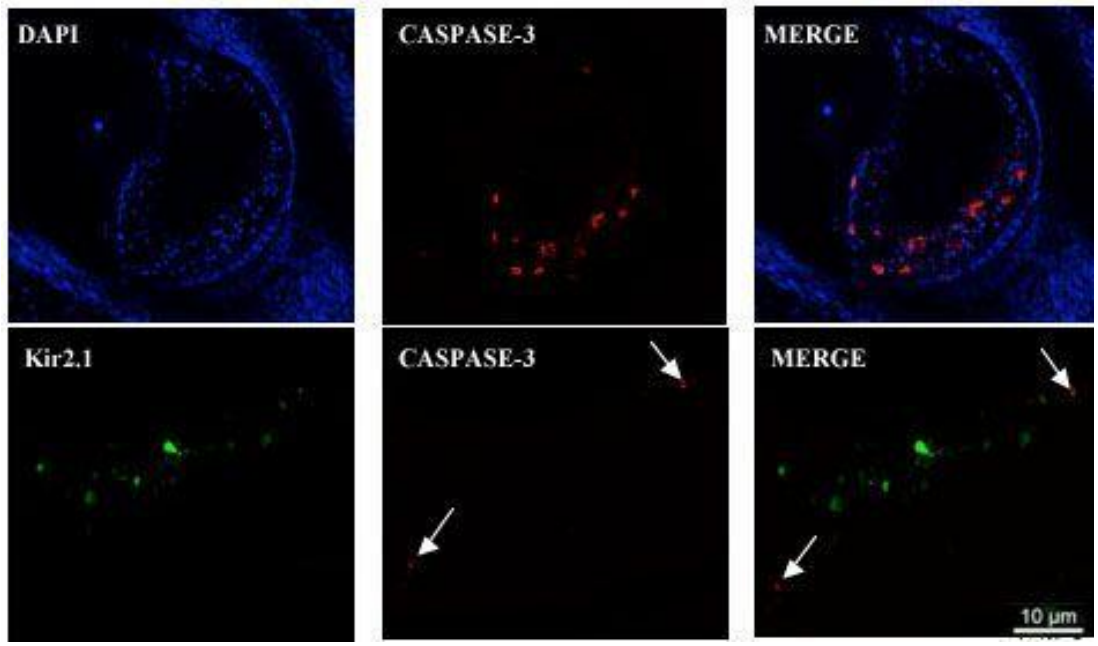

Figure 28. Cell survival is not altered after RGC activity blockade. Coronal sections of olfactory bulb (above) and electroporated RGCs expressing Kir2.1 (below) immunostained against Caspase-3. Arrows indicate Caspase-3 positive cells in the retina.

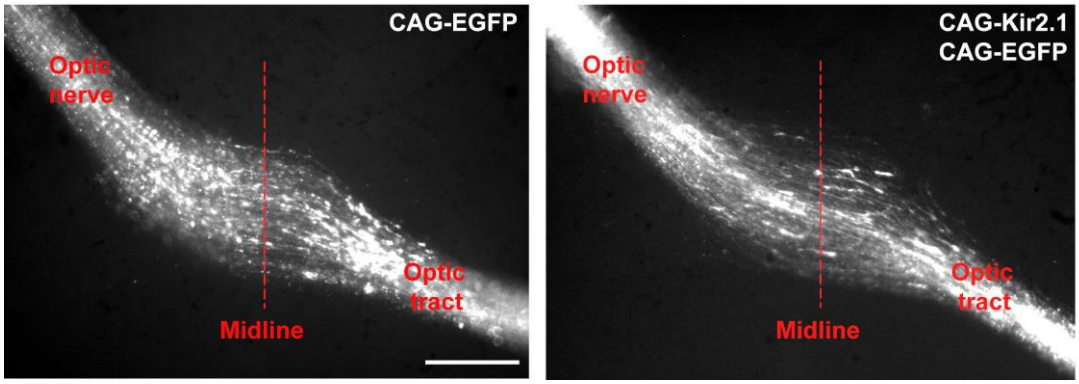

Figure 29. Axon growth and guidance are not altered after RGC activity blockade. On the left RGC axons at the optic chiasm of embryos electroporated with CAG-EGFP. On the right, RGC axons at the optic chiasm of embryos electroporated with Kir2.1. Scale bar 500 um.

After leaving the optic chiasm retinal axons continue their journey through the optic tract traversing the thalamus and finally reaching the SC. To test whether spontaneous activity is necessary for the navigation of these axons until they reach the SC at birth we have compared the SC of newborn mice electroporated with Kir2.1/EGFP or with EGFP alone. Quantification of fluorescence intensity along the R-C axis of the SC (see Materials and Methods) revealed no significant timing differences in axons reaching the most caudal area of the SC at birth between mice electroporated with Kir2.1/EGFP (n=5) or with EGFP alone (n=5).

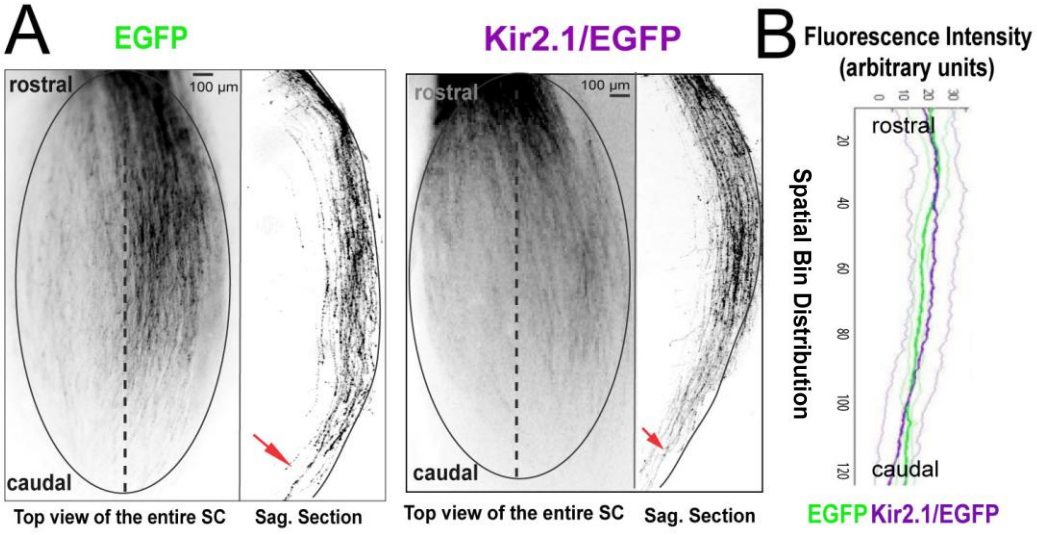

Figure 30. Axons from RGC expressing Kir2.1 correctly reach the caudal SC at birth. A. Images show a representative example of a P0 SC electroporated at E13 with Kir2.1/EGFP plasmids. On the left, top view of the SC. On the right, sagital section through the SC at the level indicated by the dotted line. Red arrows indicate the termination of the majority of the

targeted axons. **B.** Graphs on the right represent mean ± s.e.m fluorescence intensity from three consecutive sections of the SCs of five mice.

To conclude, RGCs ectopically expressing Kir2.1 did not show an increase in apoptosis. Their axons at the optic chiasms did not exhibit obvious alterations and they were able to reach the caudal SC at birth in the same extent as control RGC axons (Fig. 30), demonstrating that cell survival, axon growth and axon guidance are not altered after RGC activity blockade from early stages of development. After confirming that spontaneous activity was silenced in electroporated RGCs and after demonstrating that activity blockade does not affect cell survival, growth velocity or pathfinding, we aimed to investigate the effect of spontaneous activity in retinotopic maps development. When comparing the SCs of P9 mice electroporated with Kir2.1/EGFP to those electroporated with EGFP alone we observed that axons expressing Kir2.1/EGFP or EGFP alone projected to the central colliculus in all cases corresponding with the location of targeted RGCs in the retina.

However, after quantification of fluorescence intensity levels, we observed that the SCs of mice electroporated with Kir2.1/EGFP (n=7) exhibited less fluorescence intensity than the SC of mice electroporated with EGFP alone (n=7) (Fig. 31) despite the area of targeted RGCs was similar in both cases. Therefore these results support previous reports describing that the retinocollicular maps are disrupted after spontaneous activity blockade (O´Leary et al., 1986, Chandasekaran et al., 2005, McLaughlin et al., 2003).

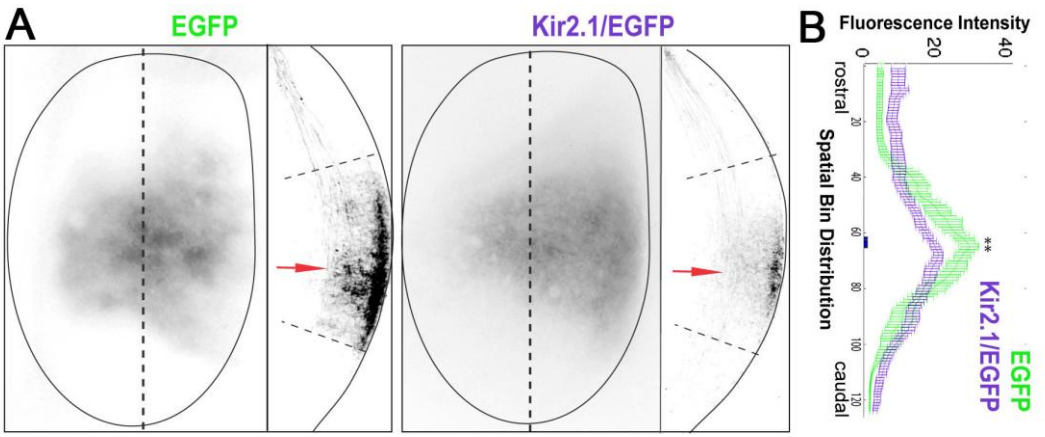

Figure 31. Activity blockade leads to disruption of the visual topographic map. A. Images show a representative example of a P9 SC electroporated at E13 with Kir2.1/EGFP plasmids. On the left, top view of the SC. On the right, sagital section through the SC at the level indicated by the dotted line. Red arrows indicate the termination zone of the targeted axons. **B.** Graphs on the right represent mean ± s.e.m fluorescence intensity from three consecutive sections of the SCs of seven electroporated mice. Red arrows point to the most intense fluorescence area in each case (**p<0.01, ANOVA-One way).

4. Retinal spontaneous activity is not required to activate EphA/ephrinA signaling during retinocollicular map formation.

In the developing spinal cord, *in vivo* alterations in the pattern of spontaneous activity affects the normal expression of EphA4 receptors in motorneurons (Hanson and Landmesser, 2004). However, in the visual system, blocking activity with TTX *in vitro* does not change the expression of EphA receptors (Nicol et al., 2007). To analyze whether activity inhibition *in vivo* affects the expression of EphA receptors in the retina we measured the levels of EphA mRNA in the retina after electroporation of Kir2.1. EphA5 and EphA6 are the only members of the EphA family expressed in a high-temporal to low-nasal gradient in the mouse retina and therefore we analyzed the endogenous levels of these receptors by quantitative RT-PCR (qRT-PCR) in E16 retinas electroporated at E13 with Kir2.1/EGFP or with EGFP alone. We used oligos against Kir2.1 mRNA as positive controls to monitor ectopic expression of Kir2.1. Our results show that, while Kir2.1 mRNA levels were highly increased in retinas

electroporated with Kir2.1/EGFP, the levels of EphA5 and EphA6 mRNA were similar to those electroporated with EGFP. So, in contrast to what happens in the spinal cord for EphA4 and in agreement with previous *in vitro* results in the retina, spontaneous ctivity is not required for the endogenous expression of retinal EphA5 or EphA6 mRNAs during retinocollicular map formation (Fig. 32).

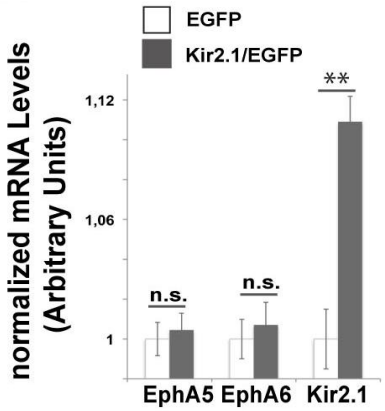

Figure 32. Spontaneous activity is not required for the endogenous expression of retinal EphA5 or EphA6 mRNAs. Graphs show mRNA levels for EphA5 and EphA6 in E16 retinas of embryos electroporated at E13 with EGFP alone or with Kir2.1/EGFP plasmids. Ten retinas for each condition were pooled per experiment. Average of four experiments is shown. Error bars indicate ± s.e.m. (**p<0.01, Student's unpaired t-test).

After confirming that endogenous expression of EphA mRNA is not affected by activity blockade we aimed to investigate whether the activation of EphA/ephrinA signaling requires spontaneous activity. Recent studies from our laboratory showed that EphA6 is the EphA receptor more abundantly expressed by temporal RGCs and that the ectopic expression of EphA6 in the mouse retina is sufficient to send axons to the rostral area of the SC by P9 (Carreres et al., 2011). However, whether RGC axons expressing EphA6 overshoot the SC at birth for posterior retraction at P9 as in natural conditions has not been analyzed yet. This was an essential issue to test in order to see whether we can use ectopic expression of EphA6 as a tool to answer whether RGC spontaneous activity is necessary for the activation of the EphA/ephrinA

signaling.

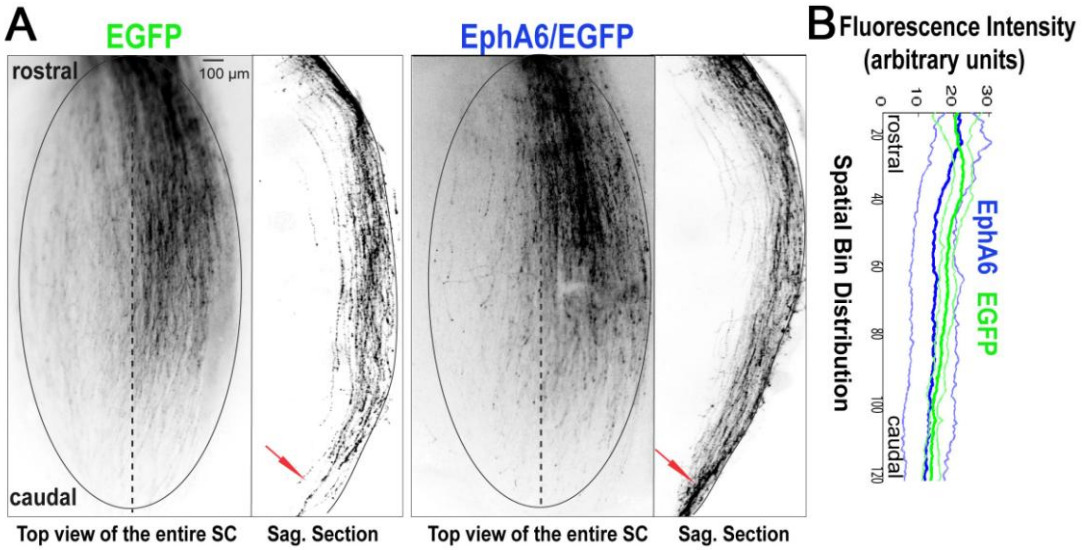

Figure 33. Ectopic expression of EphA6 in the central retina reproduces the endogenous pattern of temporal axons. A. Images show a representative example of a P0 SC electroporated at E13 with Kir2.1/EGFP plasmids. On the left, top view of the SC. On the right, sagital section through the SC at the level indicated by the dotted line. Red arrows indicate the termination of the majority of the targeted axons. **B.** Graphs on the right represent mean ± s.e.m fluorescence intensity from three consecutive sections of the SCs of five electroporated mice. Graphs on the right represent mean ± s.e.m fluorescence intensity from three consecutive sections of the SCs of electroporated mice. (ANOVA-One way test).

Plasmids bearing the coding sequence of EphA6, together with EGFP plasmids or EGFP plasmids alone were introduced into the retina by *in utero* electroporation and the SC of electroporated mice was analyzed at birth, when RGC axons normally reach the caudal colliculus. At P0, axons that ectopically express EphA6 were found in the caudal colliculus (n=5), showing a phenotype similar to that of mice electroporated with EGFP plasmids alone (n=5). Quantification of fluorescence intensity levels in both conditions revealed no significant differences between them, confirming that the ectopic expression of EphA6 in the central retina reproduces the endogenous pattern of temporal axons expressing EphA6 (Fig. 33)

Next, we electroporated EphA6 alone or Kir2.1 plus EphA6 simultaneously to

analyze if activity blockade affects EphA/ephrinA signaling. At P9, quantification of fluorescence intensity levels along the R-C axis of the SC showed that axons expressing Kir2.1/EphA6/EGFP (n=7) project into the R colliculus, showing a similar phenotype to that exhibited by axons expressing EphA6/EGFP (n=7) (Fig. 34).

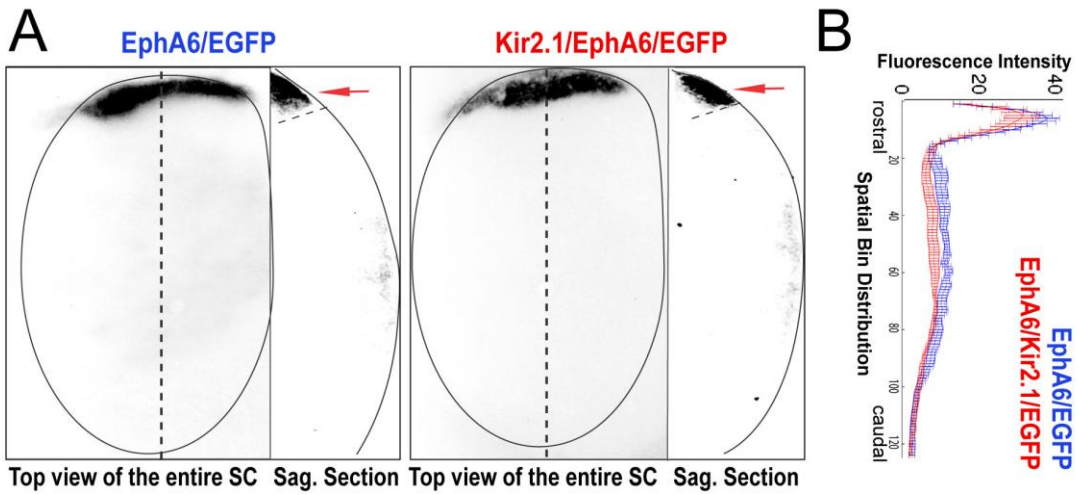

Figure 34. Spontaneous activity is not required for activating the EphA/ephrinA signalling during retinocollicular map formation. A. Images show a representative example of a P9 SC electroporated at E13 with Kir2.1/EGFP plasmids. On the left, top view of the SC. On the right, sagital section through the SC at the level indicated by the dotted line. Red arrows indicate the termination zone of the targeted axons. **B.** Graphs on the right represent mean ± s.e.m fluorescence intensity from three consecutive sections of the SCs of seven electroporated mice. Red arrows point to the most intense fluorescence area in each case (ANOVA-One way test).

These results provide the first direct evidence *in vivo* that spontaneous activity is not required for activating the EphA/ephrinA signalling that mediates the retraction of retinal axons from caudal to rostral areas of the SC during the formation of the retinocollicular map.

5. Spontaneous activity is required for local remodeling of RGC axons once they are in the correct TZ.

We have shown that spontaneous activity is not required for the activation of EphA/ephrinA signaling during retinocollicular map formation. However, we found defects in the SC of P9 mice that were electroporated with Kir2.1, indicating that activity plays a role in the formation of the retinocollicular map, as previously proposed. To further analyze the function of spontaneous activity in the formation of retinocollicular maps, we decided to electroporate E16 embryos with Kir2.1/EGFP or EGFP plasmids alone at very low concentration in order to target single RGCs and analyze individual RGC axon arbors at the SC of P9 mice.

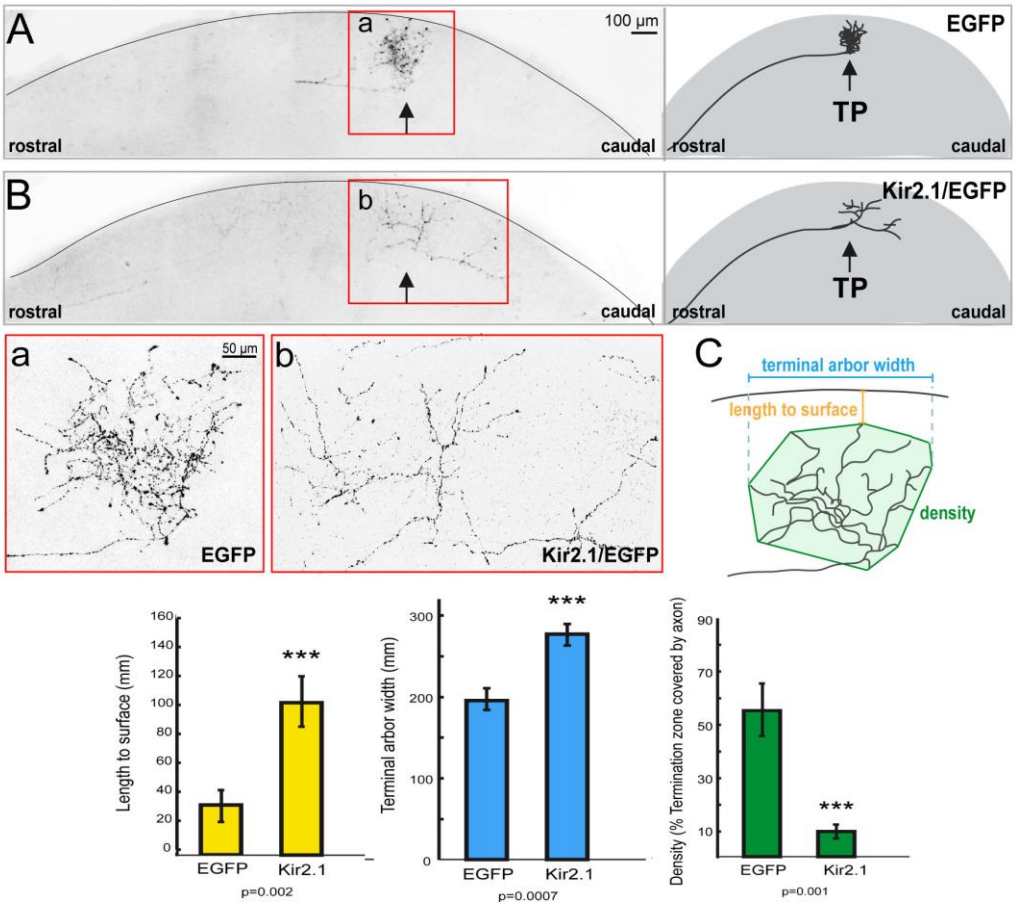

Figure 35. Spontaneous activity is required for proper remodeling of RGC axons at the TZ but not for topography. Representative sagittal sections from the SC of P9 mice electroporated at E16 with EGFP alone (**A**) or with Kir2.1/EGFP (**B**). Axons show similar turning

points (TP) (arrows) along the rostro-caudal axis of the SC in both cases, as it corresponds to the central location of their cell bodies in the retina. Right to each case, a drawing summarizes the result. **(a, b)** Close-up images of the above squared areas**. (C)** Quantification of axon branching in the SC**.** Drawing illustrating the three parameters used to measure axon terminals expressing EGFP or Kir2.1/EGFP: length to the surface, width and density. The graphs show average value of the three parameters (length, yellow; width, blue and density, green) in Kir2.1/EGFP- axons and in the controls expressing EGFP alone. Error bars represent ± s.e.m (***p<0.001, Student´s unpaired t-test).

Maximum projections derived from confocal microscopy stack scanning were used for axonal reconstructions. Quantification of single RGC axonal branching revealed that arbors from Kir2.1/EGFP expressing cells (n=8) occupy a wider termination zone area at the SC, are more distant to the surface of the SC and are less elaborated than those arbors from cells expressing EGFP alone (n=9), (Fig. 35).

However, the point along the rostrocaudal axis of the SC at which axons turn to reach their corresponding TZ was located at a similar distance from the rostral colliculus in both conditions. We also observed that collaterals outside the termination zones were rarely found in Kir2.1/EGFP or in EGFP electroporated axons (Fig. 35). In agreement with our results showing that activity is not required for the activation of EphA/ephrinA signaling, these results using electroporation to visualize individual RGCs confirm that topography is not altered in the absence of RGC spontaneous activity and definitely demonstrate that the main role of spontaneous activity in the formation of the visual circuits is local pruning and branching of RGC axons once they are in the correct TZ.

DISCUSSION

In the experiments presented in this thesis we first describe a strong correlation between neighboring RGCs *in vivo* in neonatal mice. Then, by blocking spontaneous activity in RGCs during embryonic development we show that in the visual system, spontaneous activity is not required for cell survival, growth rate or pathfinding and finally we resolve the long-standing debate about whether spontaneous activity is required to activate the EphA/ephrinA signaling during the formation of the rostrocaudal retinocollicular map.

1. Waves of spontaneous activity in the retina

In the past decade, retinal waves have been the preferred topic of developmental visual neurobiologists because the existence of these correlated activity patterns could explain the refinement of imprecise retinal projections during visual circuit formation (Chalupa, 2009). In all species studied to date, retinal waves begin before and remain after the reorganization of retinal projections.

Previous studies on the role of retinal waves during development were performed *in vitro*, using pharmacological manipulations that are highly unspecific or genetic mouse manipulations that do not completely abolish neural activity (Stafford et al., 2009). The first and to date unique recordings performed in embryonic retinas were done by Galli and Maffei (1988). These authors succeed to record embryonic RGC activity in alive pregnant rats demonstrating a high rate of correlation between pairs of neighboring RGCs. However, they did not describe the presence of retinal waves in their recordings, probably due to the poor spatial resolution of their experimental design. In later experiments performed *in vitro*, Meister et al (1991) used multielectrode arrays and calcium imaging in developing retinas and showed that RGCs and amacrine

cells became activated in the form of waves, extending across certain areas in the retina during development. We have found a clear correlation between neighboring RGCs in neonatal mice *in vivo* but have been unable to visualize retinal waves in our recordings. It is likely that the lack of waves we observe is due to our experimental conditions (anesthesia) because in the last month an elegant approach using calcium imaging *in vivo* has shown that waves of spontaneous activity are present in alive neonatal mice. Although in this study the recordings were performed in the SC and the visual cortex and not directly in the retina, their results demonstrate the existence of waves *in vivo* (Ackman et al., 2012).

2. Spontaneous activity is not required for differentiation, axon growth or pathfinding of RGCs.

In contrast to the classic view that spontaneous activity is mainly important for the refinement of axonal projections and for synaptic connections within a target (Katz and Shatz, 1996), more recently it has been attributed an essential role for spontaneous activity in several developmental processes such as cell survival, differentiation, cell migration axonal growth rate, axon pathfinding and axon targeting in different systems and models. For instance, De Marco Garcia et al., (2011) used Kir2.1 to block activity at very early stages of development in cortical differentiating neurons and observed that interneurons with blocked activity show pronounced defects in their morphologies and occupied deeper cortical layers than control cells. Thus, they concluded that early network activity has an essential role in shaping the development of specific neuronal subtypes in the central nervous system. A very recent study has also shown that ectopic expression of Kir2.1 in the thalamus causes a decrease in the growth rate that is mediated by upregulation of the guidance receptors Robo in thalamocortical axons while extending to the cortex (Mire et al., 2012). Moreover, *in-ovo* pharmacological manipulation of the systems that drive early activity has shown that motor axon pathfinding events are highly dependent on the normal pattern of bursting activity and

that alterations on activity affect the expression of guidance receptors such as EphA4 (Hanson et al., 2008). After chronic treatment with picrotoxin, which reduces the frequency of bursting episodes by half, motorneuron axons were found in inappropriate medial–lateral locations to the muscle to which they project (Hanson and Landmesser, 2004). The converse experiment, chronic treatment of chick embryos with sarcosine to increase the frequency of bursting episodes, strongly perturbed the A-P pathfinding process by which motorneurons fasciculate into pool-specific fascicles at the limb base (Hanson and Landmesser, 2006). These findings suggest that alterations in the normal patterns of neural activity in the chick embryo altered major pathfinding decisions made by motorneurons and the authors propose that precise frequency and patterning of spontaneous activity is essential in developing spinal motor circuits and that any alteration in these patterns could result in developmental defects (Kastanenka and Landmesser, 2010). Although alterations on the patterns of spontaneous activity were tested in this study, the complete abolishment of activity was not analyzed and therefore wheather spontaneous activity is needed for EphA/ephrinA signaling remains unknown.

In contrast to these early developmental defects observed in migration, growth rate and pathfinding we observed that RGCs ectopically expressing Kir2.1 showed no obvious morphological alterations and that retinal axons properly navigate through the developing brain arriving at the caudal SC at birth in the same extent as control axons did. These opposing results suggest cell-type sensitivity to changes in spontaneous activity supporting particular roles for spontaneous activity in different neural types. Alternatively, the alteration of spiking frequency in inmature motorneurons or in other cell types may be an artificial manner of affecting calcium entry that could trigger the misexpression of genes responsible for differentiation and axon guidance.

3. Spontaneous activity in the formation of the retinocollicular map.

Goodman and Shatz (1993) initially defended that in the visual system activity independent mechanisms generate a coarse topographic map relying on molecular cues, whereas the fine-tuning of this map requires patterned neural activity. Later, when spontaneous activity was described and it was obvious that these two types of mechanisms (activity-independent and activity-dependent) overlap in time, it was proposed that they could interact during development. Increasing evidence now suggest that neuronal activity and molecular cues might be linked during the formation of neural maps (Reviewed in Huberman, 2008 and Chalupa, 2009). Together with the studies showing that activity may interfere with the expression of guidance molecules early in development (Mire et al., 2012; Hanson, 2008; Handson and Landmesser, 2004; Kastanenka and Landmesser, 2010) *in vitro* studies in the visual system have suggested that spontaneous activity must be present for EphA/ephrinA signaling to act during the establishment of retinocollicular topography (Nicol et al., 2007). However blocking activity with TTX does not affect EphA transcription (Nicol et al., 2007) and our results *in vivo* confirm that the activation of the EphA/ephrinA signaling does not require spontaneous activity either.

How can we conciliate the apparent differences between *in vitro* and *in vivo* results? First of all it is important to note that there are significant differences between using TTX in culture and deliver Kir2.1 specifically in RGCs *in vivo* to block activity. In the first case, spontaneous activity is abolished in the whole coculture, including the retinal explant and the SC slide. The use of Kir2.1 however, allows blocking spontaneous activity specifically in a restricted population of RGCs leaving the rest of the retinal population and the SC unaffected. On the other hand, the organotypic retinotectal cocultures used in the *in vitro* experiments corresponded to different retinal and collicular stages. So, E15 retinas were confronted to P6 colliculi, which makes it very complicated to interpret the results since retinal axons at this early stage may not

be ready to respond to signals from a more mature SC. Finally, the resolution to distinguish between the first (topography) and the second phase (remodeling) of the maturation process using cocultures *in vitro* is very poor compared to our *in vivo* approach, in which we can easily visualize and distinguish the retraction of the principal axon and the axonal pruning and arborization in the correct TZ.

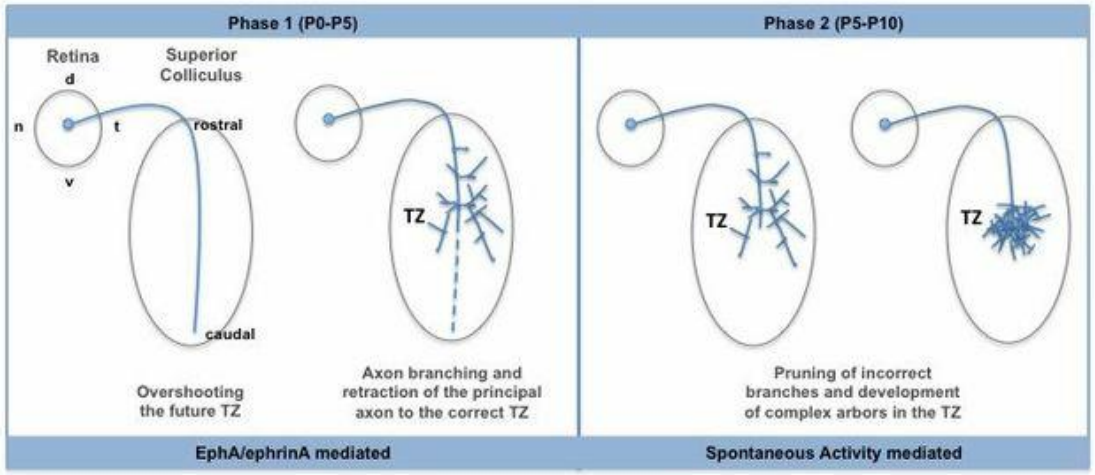

Figure 36. Drawing illustrating the two-phases process during the formation of the retinocollicular map and the main mechanisms driving each step. In the first phase topography is determined by the EphA-ephrinA signaling whereas in the second phase spontaneous activity is essential for pruning and fine-tune arborization of RGC projections once axons are located in their correct TZ.

Therefore, our *in vivo* results demonstrate for the first time that: 1) In contrast to increasing evidence obtained from other systems, spontaneous activity is not required during visual system development for cell survival, axon guidance, pathfinding, targeting, and expression of EphA receptors or activation of the EphA/ephrinA signaling, 2) Molecular guidance cues determine retinotopy by themselves in the absence of spontaneous activity, which is subsequently needed for the proper refinement of the circuits at the local level once retinal axons have reached their TZ at their visual targets. In other words, EphA-ephrinA signaling determines topography

during the first phase and spontaneous activity is essential for the fine-tune arborization and pruning of RGC arbors in the second phase of the process (Fig. 36).

In line with these results, axon arbor remodeling at the optic tectum was suppressed in zebrafish larvae after Kir2.1 overexpression in RGCs (Hua et al., 2005). However, given the reduced size of the zebrafish tectum compared to the large size of RGC arbors it was difficult to assign a role for activity to topography, arbor branching or pruning in these experiments. Our results also agree with those of Pfeiffenberger et al., 2006 and Dhande et al., 2011, showing that mice lacking β2-dependent retinal activity have nearly normal topography but fail to refine axonal arbors that appear dramatically enlarged. Even though it was later suggested that in the β2-/- mice other forms of activity (different than cholinergic activity) could be masking the role of spontaneous activity in the establishment of topography, our results discard this possibility. Finally, a very elegant approach by the laboratory of Michael Crair in which genetically modified mice with altered patterns of retinal spontaneous activity show a roughly normal R-C topography (Xu et al., 2011) also demonstrates that activity and topography are independent events.

CONCLUSIONS

CONCLUSIONS

1. *In vivo* retinal recordings confirm high correlation between neighboring retinal ganglion cells.

2. Lack of spontaneous activity in retinal ganglion cells during embryonic development does not affect cell survival, differentiation, axon growth or pathfinding.

3. Retinal spontaneous activity is not required for the expression of EphA receptors or for the activation of the EphA/ephrinA signaling during retinocollicular map formation *in vivo*.

4. Retinal spontaneous activity is needed for local arborization and pruning of RGC axons once they reach their correct termination point at the target tissue.

BIBLIOGRAPHY

BIBLIOGRAPHY

- Ackman J., B, Burbridge T., J, Crair M., C. Retinal waves coordinate patterned activity throughout the developing visual system. Nature, 2012, 490(7419):219-25.
- Allman, J. Evolving brains. Scientific American Library. 2000.
- Bansal, A., Singer, J., Hwang, B.J., Xu, W., Beaudet, A., Feller, M. Mice Lacking Specific Nicotinic Acetylcholine Receptor Subunits Exhibit Dramatically Altered Spontaneous Activity Patterns and Reveal a Limited Role for Retinal Waves in Forming ON and OFF Circuits in the Inner Retina. The Journal of Neuroscience, 2000, 20(20):7672-7681.
- Blankenship, A., G, Feller, M., B. Mechanisms underlying spontaneous patterned activity in developing neural circuits. Nature Reviews Neuroscience, 2010, 11, 18-29.
- Borrell, V., Yoshimura, Y., Callaway, E. Targeted gene delivery to telencephalic inhibitory neurons by directional in utero electroporation. Journal of Neuroscience Methods, 2005, 143 (2): p. 151-158.
- Brambilla, R., Schnapp, A., Casagranda, F., Labrador, J. P., Bergemann, A.D., Flanagan, J.G., Pasquale, F.. B, and Klein, R. Membrane-bound LERK2 ligand can signal through three different Eph-related receptor tyrosine kinases. EMBO J. 1995, 14(13): 3116–3126.
- Brunet I., Weinl C., Piper M., Trembleau A., Volovitch M., Harris W., Prochiantz A., Holt C. The transcription factor Engrailed-2 guides retinal axons. Nature. 2005 3;438(7064):94-8.

- Burrone, J., O'Byrne, M., Murthy, V., N. Multiple forms of synaptic plasticity triggered by selective suppression of activity in individual neurons. Nature, 2002, 28; 420 (6914):414-8.
- Cang J, Wang L, Stryker MP, Feldheim D., A. Roles of ephrin-as and structured activity in the development of functional maps in the superior colliculus. Journal of Neuroscience, 2008, 22; 28(43):11015-23.
- Carreres, M.,I, Escalante, A, Murillo, B, Chauvin, G, Gaspar P, Vegar, C, Herrera, E. Transcription factor Foxd1 is required for the specification of the temporal retina in mammals. Journal of Neuroscience, 2011, 13; 31(15):5673-81.
- Carvalho R., F, Beutler M., Marler K., J, Knöll B., Becker-Barroso E., Heintzmann R., Drescher U. Silencing of EphA3 through a cis interaction with ephrinA5. Nat Neurosci. 2006 (3):322-30.
- Cepko C., L, Austin C., P, Yang X., Alexiades M., Ezzeddine D. Cell fate determination in the vertebrate retina. Proc Natl Acad Sci USA, 1996, 23; 93(2):589-95.
- Chalupa, L. Retinal waves are unlikely to instruct the formation of eye-specific retinogeniculate projections. Neural Development, 2009; 4: 25.
- Chklovskii, D., B, Koulakov, A., A. Maps in the brain: What can we learn from them? Annu. Rev. Neurosci., 2004; 27:369-92.
- Chandrasekaran, A., R, Plas, D. T., Gonzalez, E., Crair, M. C. Evidence for an Instructive Role of Retinal Activity in Retinotopic Map Refinement in the Superior Colliculus of the Mouse. The Journal of Neuroscience, 2005, 25 (9): 6929-6938.
- Cohan, C., S, Kater S. B. Suppression of neurite elongation and growth cone motility by electrical activity. Science, 1986; 232(4758):1638-40.

- Constantine-Paton M., Cline H., T, Debski E. Patterned activity, synaptic convergence, and the NMDA receptor in developing visual pathways. Annu Rev Neurosci. 1990; 13:129-54.
- Cowan, C., M, Roskams A., J. Caspase-3 and caspase-9 mediate developmental apoptosis in the mouse olfactory system. Journal of Computational Neurology, 2004; 474(1):136-48.
- Cowan, C., M, Thai J., Krajewski S., Reed J., C, Nicholson D., W, Kaufmann S., H, Roskams A., J. Caspases 3 and 9 send a pro-apoptotic signal from synapse to cell body in olfactory receptor neurons. Journal of Neuroscience, 2001; 21(18):7099-109.
- Cox, E., C, Müller B., Bonhoeffer, F. Axonal guidance in the chick visual system: Posterior tectal membranes induce collapse of growth cones from the temporal retina. Neuron, 1990, Volume 4, Issue 1, Pages 31–37.
- De Marco Garcia N., V, Karayannis T., Fishell G. Neuronal activity is required for the development of specific cortical interneuron subtypes. Nature, 2011; 472(7343):351-5.
- Debski E., A, Cline H., T. Activity-dependent mapping in the retinotectal projection. Curr Opin Neurobiol. 2002 (1):93-9.
- Demyanenko G., P, Maness P., F. The L1 cell adhesion molecule is essential for topographic mapping of retinal axons. J Neurosci. 2003;23(2):530-8.
- Dhande O., S, Hua E., W, Guh E, Yeh J, Bhatt S, Zhang Y, Ruthazer ES, Feller M., B, Crair M., C. Development of single retinofugal axon arbors in normal and β2 knock-out mice. J Neurosci. 2011; 31(9):3384-99.
- Drescher, U., Kremoser, C., Handwerker, C., Löschinger, J., Noda, M., Bonhoeffer, F. In vitro guidance of retinal ganglion cell axons by RAGS, a 25 kDa tectal protein related to ligands for Eph receptor tyrosine kinases. Cell, 1995; 82(3):359-70.

- Erskine, L., Herrera, E., 2007. The retinal ganglion cell axon's journey: Insights into molecular mechanisms of axon guidance. Developmental Biology, 2007. 308 (1): p. 1-14.
- Feldheim D., A, Vanderhaeghen P, Hansen M. J, Frisén J, Lu Q. Barbacid M, Flanagan J.G. Topographic guidance labels in a sensory projection to the forebrain. Neuron, 1998; 21(6):1303-13.
- Feldheim, D. A., Kim. Y. I., Bergemann, A. D., Frisén, J. Genetic analysis of ephrin-A2 and ephrin-A5 shows their requirement in multiple aspects of retinocollicular mapping. Neuron, 2000; 25(3):563-74.
- Feldheim, D. A., O´Leary, D. M. Visual map development: Bidirectional signaling, Bifunctional guidance molecules and Competition. Cold Spring Harbor Perspectives in Biology, 2010.
- Feller, M. B., Butts, D. A., Aaron, H. L., Rokhsar, D. S., Shatz, C. J. Dynamic processes shape spatiotemporal properties of retinal waves. Neuron, 1997; 19 (2):293-306.
- Flanagan J., G. Neural map specification by gradients. Curr Opin Neurobiol. 2006; 16 (1):59-66.
- Frisén J., Yates P., A, McLaughlin T., Friedman G., C, O'Leary D., D, Barbacid M.

  Ephrin-A5 (AL-1/RAGS) is essential for proper retinal axon guidance and topographic mapping in the mammalian visual system. Neuron. 1998;20(2):235-43.
- Gale, N., W, Holland, S., J, Valenzuela, D., M, Flenniken, A., Pan, L., Ryan, T., E, Henkemeyer, M., Strebhardt, K., Hirai, H., Wilkinson, D., G. Pawson, T., Davis, S., Yancopoulos, G., D. Eph Receptors and Ligands Comprise Two Major Specificity Subclasses and Are Reciprocally Compartmentalized during Embryogenesis. Neuron, 1996, 17(1): 9-19.

- Galli, L., Lamberto, M. Spontaneous Impulse Activity of Rat Retinal Ganglion Cells in Prenatal Life. Science, 1988. 2424(875): 90-91.
- Galli-Resta, L., Ensini, M. Fusco, E., Gravina, A., and Margheritti, B. Afferent Spontaneous Electrical Activity Promotes the Survival of Target Cells in the Developing Retinotectal System of the Rat. The Journal of Neuroscience, 1993, 13 (1): 243-250.
- Garcia-Frigola**, C.** Carreres**,** M., I, Vegar, C, and Herrera, E. Gene delivery into mouse retinal ganglion cells by in utero electroporation. BMC Developmental Biology, *2007, **7**:103*
- Garcia-Frigola, C., Carreres, M., I. Vegar, C., Mason, C., and Herrera, E. Zic2 promotes axonal divergence at the optic chiasm midline by EphB1-dependent and -independent mechanisms. Development, 2008, 135 (10): 1833-1841.
- Godement P., Salaün J., Imbert M. Prenatal and postnatal development of retinogeniculate and retinocollicular projections in the mouse. J Comp Neurol. 1984; 230(4):552-75.
- Goldshmit, Y., McLenachan, S., Turnley, A. Roles of Eph receptors and ephrins in the normal and damaged adult CNS. Brain Research Reviews, 2006, Volume 52, Issue 2, Pages 327–345
- Goodman, C., S, Shatz, C., J. Developmental mechanisms that generate precise patterns of neuronal connectivity. Cell, 1993, Vol. 10 77-99.
- Hanson M., G, Landmesser L., T. Normal patterns of spontaneous activity are required for correct motor axon guidance and the expression of specific guidance molecules. Neuron, 2004;43(5):687-701.
- Hanson, M., G, and Landmesser, L., T. Increasing the Frequency of Spontaneous Rhythmic Activity Disrupts Pool-Specific Axon Fasciculation and

Pathfinding of Embryonic Spinal Motorneurons. The Journal of Neuroscience (6) 2006: 12769-12780.

- Hanson, M., G, Milner, L. D., Landmesser, T., L. Spontaneous rhythmic activity in early chick spinal cord influences distinct motor axon pathfinding decisions. Brain Res Rev, 2008. Volume 57, Issue 1, pages 77 – 85.
- Harris, W., A, Holt, C., E, Bonhoeffer, F. Retinal axons with and without their somata, growing to and arborizing in the tectum of Xenopus embryos: a time-lapse video study of single fibers in vivo. Development, 1987; 101(1):123-33.
- Hindges, R., McLaughlin, T., Genoud, N., Henkemeyer, M. & O'Leary, D.D.M. EphB forward signaling controls directional branch extension and arborization required for dorsal ventral retinotopic mapping. Neuron, 2002, 35: 475-487.
- Holcomb J., D, Mumm J., S, Calof A., L. Apoptosis in the neuronal lineage of the mouse olfactory epithelium: regulation in vivo and in vitro. Dev Biol. 1995; 172(1):307-23.
- Hua J., Y, Smear M., C, Baier H., Smith S., J. Regulation of axon growth in vivo by activity-based competition. Nature, 2005; 434(7036): 1022-6.
- Hubel, D., H. Eye, Brain, and Vision. 1988. Scientific American Library.
- Huberman A. D, Feller M. B, Chapman B. Mechanisms underlying development of visual maps and receptive fields. Annu Rev Neurosci. 2008; 31: 479-509.
- Huberman, and Niell. What can mice tell us about how vision works? Trends in Neurosciences, 2011, Volume 34, Issue 9, Pages 464–473.
- Kaas J., H. Topographic maps are fundamental to sensory processing. Brain Res Bull. 1997; 44(2):107-12.

- Kaethner R., J, Stuermer C., A. Dynamics of terminal arbor formation and target approach of retinotectal axons in living zebrafish embryos: a time-lapse study of single axons. J Neurosci. 1992;12(8):3257-71.
- Kastanenka K., V, Landmesser L., T. In vivo activation of channelrhodopsin-2 reveals that normal patterns of spontaneous activity are required for motorneuron guidance and maintenance of guidance molecules.J Neurosci. 2010; 30 (31):10575-85.
- Knöll B., Drescher U. Ephrin-As as receptors in topographic projections. Trends Neurosci. 2002; 25(3):145-9.
- Lemke' G., and Reber, M. Retinotectal mapping: New Insights from Molecular Genetics Annual Review of Cell and Developmental Biology, 2005. Vol. 21: 551-580 2005.
- Marcus R.,C, Gale N., W, Morrison M., E, Mason C., A, Yancopoulos G.,D. Eph family receptors and their ligands distribute in opposing gradients in the developing mouse retina. Dev Biol. 1996;180(2):786-9.
- McLaughlin, D.M., Feller, M., Tornborg, C.L., and O´Leary, T. Retinotopic Map Refinement Requires Spontaneous Retinal Waves during a Brief Critical Period of Development, Neuron, 2003. 40 (6): p. 1147-1160.
- McLaughlin, T., O´Leary, D., M. Molecular gradients and development of retinotopic maps. Annual Review of Neuroscience, 2005. 28: p. 327-355.
- Meister, M., Wong, R. O., Baylor, D. A., Shatz, C. J. Synchronous bursts of action potentials in ganglion cells of the developing mammalian retina. Science, 1991; 252 (5008): 939-43.
- Miller, E., Wong, O.L., Myhr, K. Developmental Changes in the Neurotransmitter Regulation of Correlated Spontaneous Retinal Activity. The Journal of Neuroscience, 1999, 20 (1): p. 351-360.

- Mire, E., Mezzera, C., Leyva-Díaz, E., Paternain, A., Squarzoni, P., Bluy, L., Castillo-Paterna, M., López, M. J., Peregrín, S., Tessier-Lavigne, M., Garel, S., Galcerán, J., Lerma, J., López-Bendito, G. Spontaneous activity regulates Robo1 transcription to mediate a switch in thalamocortical axon growth. *Nature Neuroscience,* 2012, 15, 1134–1143.
- Mui, S. H., Hindges, R., O'Leary, D. M., Lemke, G., Bertuzzi, S. The homeodomain protein Vax2 patterns the dorsoventral and nasotemporal axes of the eye. Development 129, 797-804.
- Nakamoto M., Cheng H., J, Friedman G., C, McLaughlin T., Hansen M., J, Yoon C., H, O'Leary D., D, Flanagan J.,G. Topographically specific effects of ELF-1 on retinal axon guidance in vitro and retinal axon mapping in vivo. Cell, 1996; 86(5): 755-66.
- Nakamura, H., O'Leary, D., D. Inaccuracies in initial growth and arborization of chick retinotectal axons followed by course corrections and axon remodeling to develop topographic order. The Journal of Neuroscience, 1989; 9(11):3776-95.
- Nichols, C., Lopatin, A. Inward rectifier potassium channels. Annual review of psysiology, 1997, 59: p. 171-191.
- Nicol X., Muzerelle A., Rio J., P, Métin C., Gaspar P. Requirement of adenylate cyclase 1 for the ephrin-A5-dependent retraction of exuberant retinal axons. J Neurosci. 2006;26(3):862-72.
- Nicol, X., Voyatzis, S. Muzerelle, A., Narboux-Nême, N., Südhof, T., Miles, R. cAMP oscillations and retinal activity are permissive for ephrin signaling during the establishment of the retinotopic map. Nature Neuroscience, 2007, *10*, 340 – 347.
- O´Leary., D, Fawcett, J., Cowan, W. Topographic targeting errors in the retinocollicular projection and their elimination by selective ganglion cell death. Journal of Neuroscience, 1986, 6, p. 3692-3705.

- O'Rourke**,** A., Cline, H., Fraser, S**.** Rapid remodeling of retinal arbors in the tectum with and without blockade of synaptic transmission. Neuron, Volume 12, Issue 4, 921-934, 1994.
- Pfeiffenberger, C., Cutforth, T., Woods, G., Yamada, J., Rentería, R., C. Copenhagen, D., R. Flanagan, J., G. & Feldheim, D., A. Ephrin-As and neural activity are required for eye-specific patterning during retinogeniculate mapping. Nature Neuroscience, 2005, 8, 1022 - 1027.
- Plas, D., T, Visel, A., Gonzalez, E., She, W., C, Crair, M., C. Adenylate Cyclase 1 dependent refinement of retinotopic maps in the mouse, Vision Research, 2004, Volume 44, Issue 28, Pages 3357–3364.
- Purves, D., Augustine, G. J., Fitzpatrick, D., WC Hal. Neuroscience, 2008 - Sinauer Associates.
- Rashid T., Upton A., L, Blentic A., Ciossek T., Knöll B., Thompson I., D, Drescher U. Opposing gradients of ephrin-As and EphA7 in the superior colliculus are essential for topographic mapping in the mammalian visual system. Neuron. 2005;47(1):57-69.
- Saito, T., Nakatsuji, N. Efficient Gene Transfer into the Embryonic Mouse Brain Using in Vivo Electroporation. Developmental Biology, 2001, 240 (1): p. 237-246.
- Scicolone G., Ortalli A.,L, Carri N.,G. Key roles of Ephs and ephrins in retinotectal topographic map formation. Brain Res Bull. 2009; 79(5): 227-47.
- Schmitt A., M, Shi J., Wolf A., M, Lu C., C, King L., A, Zou Y. Wnt-Ryk signalling mediates medial-lateral retinotectal topographic mapping. Nature. 2006;439(7072):31-7.
- Shatz C., J. Competitive interactions between retinal ganglion cells during prenatal development. J Neurobiol. 1990; 21(1): 197-211.

- Shatz, C., J. Emergence of order in visual system development Journal of Physiology Paris, 1996; 90(3-4): 141-50.
- Shigetani Y., Funahashi J., I, Nakamura H. En-2 regulates the expression of the ligands for Eph type tyrosine kinases in chick embryonic tectum. Neurosci Res. 1997;27(3):211-7.
- Sperry, R., W. Chemoaffinity in the orderly growth of nerve fiber patterns and connections. Proc Natl Acad Sci U S A. 1963; 50(4): 703–710.
- Spitzer, N., C. Electrical activity in early neuronal development, *Nature* 2006, 444, 707-712.
- Stafford, B., K, Sher, A., Litke, A., M. Feldheim, D., A. Spatial-temporal patterns of retinal waves underlying activity-dependent refinement of retinofugal projections. Neuron, 2009; 64(2):200-12.
- Stahl, B., Müller, Y, von Boxberg, E., Cox, C., Bonhoeffer, F. Biochemical characterization of a putative axonal guidance molecule of the chick visual system. Neuron, 1990; 5(5):735-43.
- Stellwagen, D., Shatz, C., Feller, M., Dynamics of Retinal Waves Are Controlled by CyclicAMP, Neuron, 1999, 24 (3): P. 673-685.
- Stosiek, C.,Garaschuk,O., Holthoff,K., Konnerth, A. In vivo two-photon calcium imaging of neuronal networks, The National Academy of Sciences, 2003, 100 (12): p. 7319-7324.
- Torborg, C., L, Feller, M., B. Spontaneous patterned retinal activity and the refinement of retinal projections. Progress in neurobiology, 2005; 76(4):213-35.
- Uesaka, N., Hirai, S., Maruyama T., Ruthazer , E. S., Yamamoto, N. Activity dependence of cortical axon branch formation: a morphological and electrophysiological study using organotypic slice cultures. J Neurosci. 2005; 25(1):1-9.

- Walter, J., Henke- Fahle, S., Bonhoeffer, F. Avoidance of posterior tectal membranes by temporal retinal axons. Development, 1987, 101, 909-913.
- Wilkinson D., G. Topographic mapping: organising by repulsion and competition? Curr Biol. 2000;10(12):R447-51.
- Wong, R. Retinal waves and visual system development. Annual Review of Neuroscience, 1999. 22: p.29-47.
- Yamada A., Uesaka N., Hayano Y., Tabata T., Kano M., Yamamoto N. Role of pre- and postsynaptic activity in thalamocortical axon branching. Proc Natl Acad Sci USA, 2010; 107(16):7562-7.